INTERNATIONAL CENTER FOR AGGREGATES RESEARCH

ICAR

CHARACTERIZATION OF AGGREGATE RESISTANCE TO DEGRADATION IN STONE MATRIX ASPHALT MIXTURES

RESEARCH REPORT ICAR – 204-1F

Sponsored by the
Aggregates Foundation
for Technology, Research and Education

1. Report No.	2. Government Accession No.	3. Recipient's Catalog No.
ICAR/204-1F		

4. Title and Subtitle	5. Report Date
CHARACTERIZATION OF AGGREGATE RESISTANCE TO DEGRADATION IN STONE MATRIX ASPHALT MIXTURES	July 2006
	6. Performing Organization Code

7. Author(s)	8. Performing Organization Report No.
Dennis Gatchalian, Eyad Masad, Arif Chowdhury and Dallas Little	Report No. 204-1F

9. Performing Organization Name and Address	10. Work Unit No. (TRAIS)
Texas Transportation Institute The Texas A&M University System College Station, Texas 77843-3135	11. Contract or Grant No. Project No. 400901

12. Sponsoring Agency Name and Address	13. Type of Report and Period Covered
Aggregates Foundation for Technology, Research, and Education 1605 King Street Arlington, VA 22314	Final- July 2006
	14. Sponsoring Agency Code

15. Supplementary Notes

Research performed in cooperation with International Center for Aggregates Research and Aggregates Foundation for Technology, Research, and Education.
Research Project Title: Role of Aggregate Characteristics on Resistance to Load in SMA

16. Abstract

Stone matrix asphalt (SMA) mixtures rely on stone-on-stone contacts among particles to resist applied forces and permanent deformation. Aggregates in SMA should resist degradation (fracture and abrasion) under high stresses at the contact points. This study utilizes conventional techniques as well as advanced imaging techniques to evaluate aggregate characteristics and their resistance to degradation. Aggregates from different sources and types with various shape characteristics were used in this study. The Micro-Deval test was used to measure aggregate resistance to abrasion. The aggregate imaging system (AIMS) was then used to examine the changes in aggregate characteristics caused by abrasion forces in the Micro-Deval.

The resistance of aggregates to degradation in SMA was evaluated through the analysis of aggregate gradation before and after compaction using conventional mechanical sieve analysis and nondestructive X-ray computed tomography (CT). The findings of this study led to the development of an approach for the evaluation of aggregate resistance to degradation in SMA. This approach measures aggregate degradation in terms of abrasion, breakage, and loss of texture.

•

17. Key Words	18. Distribution Statement
Aggregate degradation, Aggregate Shape, Angularity, Texture, SMA Imaging, and AIMS.	No restrictions. This document is available to the public through NTIS: National Technical Information Service 5285 Port Royal Road Springfield, Virginia 22161

19. Security Classif.(of this report)	20. Security Classif.(of this page)	21. No. of Pages	22. Price
Unclassified	Unclassified	120	

Form DOT F 1700.7 (8-72) Reproduction of completed page authorize

ROLE OF AGGREGATE CHARACTERISTICS IN RESISTANCE TO LOAD IN SMA

by

Dennis Gatchalian
Graduate Research Assistant
Texas A&M University

Eyad Masad
E.B. Snead I Associate Professor
Texas A&M University

Arif Chowdhury
Associate Transportation Researcher

and

Dallas Little
Senior Research Fellow
Texas A&M University

Report No 204-1

Project No. 400901
Research Project Title: Role of Aggregate Characteristics to Load in SMA

Sponsored by
Aggregate Foundation for Technology, Research, and Education

August 2006

Texas A&M University
TEXAS TRANSPORTATION INSITUTE
College Station, Texas 77840
MS 3135

TABLE OF CONTENTS

LIST OF TABLES

LIST OF FIGURES

CHAPTER I

INTRODUCTION

Problem Statement

The use of stone matrix asphalt (SMA) has steadily increased since its introduction in the United States in 1991 (*1*). This mix provides engineers with another alternative in the search of a more rut-resistant and cost-effective asphalt mixture. Prior to its introduction in the U.S., it was originally developed in Europe to resist studded tire wear. However it has also been used to successfully minimize rutting and lower maintenance costs in high traffic areas throughout Europe, in particular Germany (*2*).

Aggregate structure in SMA plays a significant role in the resistance of the mix to permanent deformation. The structure is dependent on the stone-on-stone contacts of the coarse aggregate in the mix (*1,3*), which places demands on aggregates that are different from those in conventional continuously graded mixtures. Conventional dense-graded mixtures often allow coarse aggregates to essentially "float" in a matrix of fine aggregates and asphalt binder; therefore, in these conventional mixes, strength properties of coarse aggregates are less important. Currently, there is no test to directly measure this type of interaction. In SMA, the existence of stone-on-stone contact is evaluated by measuring the voids in the coarse aggregate (VCA). Stone-on-stone contact is established by ensuring that the VCA of the mixture is less than the VCA of the coarse aggregate by means of the dry rodded test (*4*). Although this procedure is used to ensure stone-on-stone contact, it is an indirect indication of the existence of aggregate contacts.

No direct methods exist in hot mixed asphalt (HMA) or SMA mix design procedures that measure the resistance of aggregates to sustain contact stresses among coarse aggregate particles.

Evidence indicates that construction operations, particularly compaction of thin layers, plus subsequent traffic loadings can contribute to degradation of coarse aggregates at the contact points, which can significantly alter the original design gradation and create uncoated aggregate faces. Broken binder films can also provide inlets for water, which, in concert with traffic loads, can exacerbate stripping. Therefore, strength properties of coarse aggregates are clearly more significant in SMA mixtures when compared with conventional mixtures.

Selection of aggregate for SMA is an important factor in the development of a mixture design. There is a need to develop methods that are capable of predicting the ability of aggregates to withstand high contact stresses within the aggregate structure without significant breakage of particles. The lack of such methods has caused some state highway agencies to require superior aggregates to be used in SMA without rational methods to measure the properties of these aggregates. The emphasis of using a superior aggregate in SMA overshadowed the development of a design method that accommodates a wide array of aggregates. Because the performance of SMA is dependent on the aggregate, it is important to analyze and select aggregates based on their characteristics and performance. A method is needed to determine whether an aggregate is suitable to handle the demands required of SMA.

It is imperative that the contribution of aggregate strength to the behavior of SMA mixes under loading is understood and that methods are developed to measure this contribution before significant problems are created. Recently, new methodologies to evaluate the aggregate structure in asphalt mixtures have been developed (*5-12*). Most of these studies focus on measuring stone-on-stone contact within an SMA specimen by analyzing the VCA of the mixtures. Some of these studies incorporate imaging technology to measure aggregate properties, breakdown, and aggregate contact in SMA mixtures (*9,12*).

Objectives of the Study

To understand the relationship of aggregate properties and SMA performance, several analysis methods to evaluate aggregate properties and their interaction in SMA are explored. These methods should be able to determine the properties of aggregates such as shape, texture, angularity, and resistance to degradation. Also, methods should measure aggregate degradation under compaction and repeated loading. In addition, the analysis techniques should be applicable to both field samples and laboratory specimens, which can establish a connection between aggregate properties, mix design, compaction and SMA performance.

Essentially, the main objectives of this study are to characterize the resistance of aggregates to degradation (abrasion and fracture) in SMA mixtures and recommend test methods to measure aggregate properties related to their resistance. The objectives described will be achieved through completion of the following tasks:

- Design SMA mixtures using different aggregate sources,
- Measure aggregate properties such as abrasion resistance and physical characteristics,
- Observe aggregate structure stability during compaction,
- Quantify aggregate degradation due to compaction using different conventional and advanced methods such as X-ray Computed Tomography (CT),
- Quantify aggregate degradation due to repeated dynamic loading, and
- Recommend an approach for the selection of aggregates in SMA.

Report Organization

This report is organized into the following six chapters:

- Chapter I provides an introduction to the problem statement and motivation of this research, followed by the objectives of the study and a brief overview of the report layout.
- Chapter II presents the literature review on the topics related to the study. It provides a brief background on stone matrix asphalt and describes several methods used in this study to analyze SMA.
- Chapter III introduces the experimental setup used in this study. The materials and mixture designs and several experimental methods that are used to analyze aggregate degradation are described.
- Chapter IV presents the results that are obtained in the study. Analysis of results and correlation of the data are further discussed in this chapter.

- Chapter V provides the conclusions and any recommendations provided by the researcher. Furthermore, discussion of future research is also introduced.

CHAPTER II

BACKGROUND

This chapter provides some background on SMA, a description of the aggregate requirements for SMA, an explanation of the methodology used to measure the aggregate structure in SMA, and a discussion of several methodologies used to characterize the properties of aggregates used in SMA mixtures.

Description of SMA

SMA was developed in the 1960s as a means to reduce the wear and damage due to studded tire use in Germany. Its original popularity decreased in the 1970s due to the illegalization of studded tires in Germany and the increase in material and construction costs associated with the mixture (*1*). However, countries like Sweden continued using SMA with great success because of its rut-resistant nature provided by its coarse aggregate structure (*3*). Eventually, other countries also adopted SMA to provide a solution for increasing wheel loads and traffic volumes. Several case studies have also reported that SMA mixtures exhibit very good resistance to rutting and perform as well as or better than Superpave mixtures (*2,13 – 15*).

The rut-resistant nature of SMA is a result of stone-on-stone contacts within the aggregate structure. It is a gap-graded mixture that contains a large amount of coarse aggregates, some fine aggregate, high filler content, asphalt binder, and cellulose fiber.

Typical SMA mixtures retain approximately 70 percent of their coarse aggregate on or above the 2.36 mm (#8) sieve. Furthermore, the filler in SMA typically consists of 10 percent passing the 0.075 mm (#200) sieve (*1*). Cellulose fiber is often added to prevent draindown in the mixture due to the high asphalt content typically found in SMA, which can result in fat spots on the pavement surface (*10*).

In 1990, the European Asphalt Study Tour involved a group of U.S. pavement specialists that traveled to Europe to investigate their pavements and asphalt technologies; one of these technologies was SMA (*16*). As a result of the tour, it was decided that several trial sections of SMA should be constructed in the U.S. (*1*). The first trial section was built in Wisconsin along Interstate 94, near Milwaukee (*17*).

The use of SMA has increased since the first installations of the trial sections in the early 1990s. Although the popularity of SMA has increased in the U.S. since the installation of the trial sections, mixture designs are still derived from their European counterparts. There still is no method to predict the performance of SMA, let alone establish a mixture design.

Aggregate Requirements in Stone Matrix Asphalt

In 1994, a study by Brown and Mallick (*10*) explored the relationship between SMA properties and mixture design. One of the issues that this study had addressed was the experimental determination of stone-on-stone contact and draindown. The researchers found that by plotting both the VCA and the voids in the mineral aggregate (VMA), stone-on-stone contact could be identified. Essentially, the suggested method

determines that stone-on-stone contact is achieved when the VCA of the asphalt mixture after compaction is less than or equal to the VCA of the coarse aggregate (VCA_{DRC}) portion of the total aggregate blend (*8*). Another study by Brown and Mallick (*18*) examined the relationship of VMA and VCA and analyzed two other methods that determined the mixture stability due to aggregate contacts.

A paper discussing the development of the first mixture design procedure for SMA was published in 1997 (*7*). This was the basis for the AASHTO design specifications listed in MP8 and PP41 (*4*). Further details of their results can be found in Brown (*1*) and Brown and Mallick (*10*). Recommendations for coarse aggregate selection for SMA are presented in Table 2.1.

Table 2.1 Coarse Aggregate Quality Requirements (AASHTO MP8-01).

Test	Method (AASHTO)	Specification	
		Minimum	Maximum
Los Angeles (L.A.) Abrasion, % Loss	T96	-	30
Flat and Elongated, %			
3:1	D4791	-	20
5:1	D4791	-	5
Absorption, %	T85	-	2.0
Crushed Content, %	D5821		
1-Face		100	-
2-Face		90	-

The researchers recommended the Los Angeles (L.A.) abrasion test to determine aggregate toughness and suggested that cubical aggregates are more appropriate for SMA (*7*). SMA demands tough aggregates to ensure aggregate contacts and the rut

resistant characteristics of the mixture. The specification only allows a small fraction of flat and elongated particles (F+E) in the mixture. The limitation of the percentage of flat and elongated particles is based on previous studies that showed flat and elongated aggregates exhibit increased aggregate degradation as opposed to cubical aggregates (*6*,*19*,*20*).

Unfortunately, there are no current specifications that address the influence of aggregate shape characteristics (i.e. texture and angularity) and resistance to abrasion on the degradation of aggregates under the high stresses at contact points in SMA.

Measurements of Aggregate Structure in SMA

The aggregate structure in SMA is an important factor that makes this mixture resistant to rutting. Therefore, the ability to measure the stability of the aggregate structure is crucial to ensure the proper design of a mixture. Several methods are currently used to ensure the achievement of a stable aggregate structure that can resist deformation. Review of these studies and their findings will be presented in the following sections.

Measurement of Aggregate Structure Stability during Compaction

The Contact Energy Index (CEI) is a measure of HMA stability after compaction in the Servopac gyratory compactor (SGC). The CEI indicates the ability of an asphalt mixture to develop aggregate contacts and resist shear deformation (*21*). CEI is the

product of the shear force in the mix and the deformation during compaction. Dessouky et al. (*21,22*) developed the equations to calculate the shear force in the mix as follows:

$$S_\theta = (N_2 - N_1)\cos\theta + \frac{1}{2}\left(\sum P - W_d\right)\tan\theta + \frac{\left(N_2 - N_1\right)\sin^2\theta}{\cos\theta} \quad (2.1)$$

$$N_2 - N_1 = \frac{\left(A + \frac{W_m}{2}\right)\left(x_\theta - \frac{h}{2}\tan\theta\right) - \frac{1}{2}\left(\sum P - W_d\right)\left(x_\theta - \frac{r}{\mu}\tan\theta\right)}{\frac{h}{4\cos\theta} + \mu r\cos\theta - r\left(\frac{\sin^2\theta}{\mu\cos\theta}\right)} \quad (2.2)$$

Where:

S_θ = shear force

P_i = the forces of the actuators (i = 1, 2, 3)

W_m = weight of the asphalt mix

W_d = weight of the mold

A = resultant force of the upper pressure applied by the upper actuator

θ = angle of gyration (degrees)

h = specimen height

r = specimen radius

N_i = normal force acting on half the specimen surface

μ = friction factor

$$CEI = \sum_{N_1}^{N_2} S_{N\theta} d_e \quad (2.3)$$

Where:

d_e = change in height at each gyration

Dessouky et al. analyzed the relationship among CEI and mixture design and aggregate properties. Two types of aggregates were used in the study: limestone and gravel. In addition, natural sand was used as well as different asphalt contents. The researchers found that the mixture design properties of HMA such as aggregate size, gradation, aggregate source, and asphalt content do affect the CEI value. Specifically, the study reported lower CEI values for mixtures that contained natural sand, higher asphalt contents, and smooth aggregates.

Bahia et al. (*23*) also conducted a study to analyze several methods to investigate asphalt mixture stability during compaction. Their study showed that CEI increased with addition of manufactured sands. Furthermore, Bahia et al. did not report a consistent relationship between asphalt content and CEI as opposed to the findings by Dessouky et al.

Verification of Stone-on-Stone Contact with VCA Testing

The current method to ensure the existence of stone-on-stone contacts in SMA relies on performing the VCA test. As mentioned earlier, this methodology compares VCA_{DRC} with the VCA of the asphalt mixture after compaction. The values for VCA_{DRC} are determined using the following equation (*AASHTO T19*):

$$VCA_{DRC} = \left[\frac{\left(G_{CA}\gamma_W - \gamma_S \right)}{G_{CA}\gamma_W} \right] 100 \qquad (2.4)$$

Where,

G_{CA} = Bulk specific gravity of the coarse aggregate

γ_W = Unit weight of water (998kg/m^3)

γ_S = Unit weight of the coarse aggregate fraction of the aggregate blend

$$VCA_{MIX} = 100 - \left(\frac{G_{MB}}{G_{CA}} P_{CA} \right) \quad (2.5)$$

Where,

G_{MB} = Bulk specific gravity of mix

G_{CA} = Bulk specific gravity of the coarse aggregate

P_{CA} = Percent of coarse aggregate (retained on breakpoint sieve) by weight of total mix

The VCA of the asphalt mixture (VCA_{MIX}) is determined using Equation 2.5. The percent of coarse aggregate (PCA) is dependent on the breakpoint sieve of the respective asphalt mixture used. It was found for 9.5 mm mixtures that the breakpoint sieve was the 2.36 mm (#8) rather than the 4.75 mm (#4), which is used for larger nominal maximum aggregate size mixtures as previously observed (*9*). Once both values are determined, VCA_{MIX} must be less than the VCA_{DRC} to ensure that stone-on-stone contact exists. If the VCA_{MIX} is greater than the VCA_{DRC}, it is assumed that aggregate contact does not exist. Brown and Haddock (*8*) report that this can occur if the coarse aggregate breaking down which results in aggregates that pass through the #4 sieve. Essentially, it is very important to observe the VCA, as it directly affects whether aggregate contact exists in SMA.

Evidence of Aggregate Degradation in SMA

A laboratory study conducted by Xie and Watson (*6*) reported experimental evidence of aggregate degradation in SMA mixtures. Specifically, the focus of the study was to track aggregate breakdown due to compaction using the Superpave Gyratory Compactor (SGC) and the Marshall hammer. Furthermore, the influence of L.A. abrasion value and F&E content on the change of aggregate gradation was examined. They found that aggregates experienced breakdown due to compaction; however, the Marshall hammer exhibited more aggregate breakdown, as can be seen on Figure 2.1 through comparing the gradation after compaction with that before compaction.

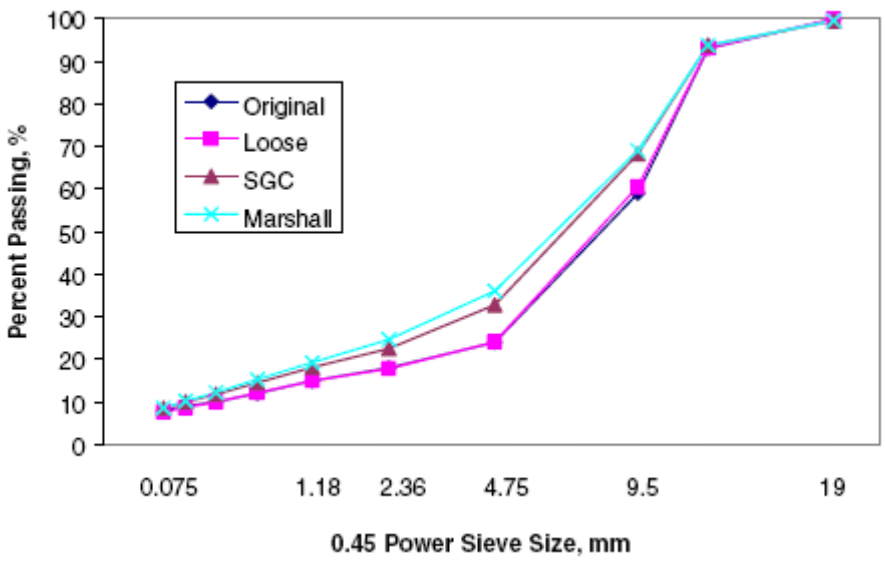

Figure 2.1: Influence of Compaction on Change in Gradation (after Xie and Watson 2004).

The L.A. abrasion value and F&E content were found to affect the amount of aggregate degradation that occurred during compaction. The higher the L.A. abrasion

value and/or F&E was, the more aggregate degradation was measured. Figures 2.2 and 2.3 show the correlations of L.A. abrasion value and F&E value with aggregate breakdown measured as the change in percent of aggregate passing the 4.75 mm (#4) sieve. Xie and Watson demonstrated that aggregate degradation is an important factor to consider when selecting aggregates for use in SMA. They emphasized that selecting an aggregate that has a low L.A. abrasion value and controlling the percent of F&E aggregates, can minimize aggregate degradation potential.

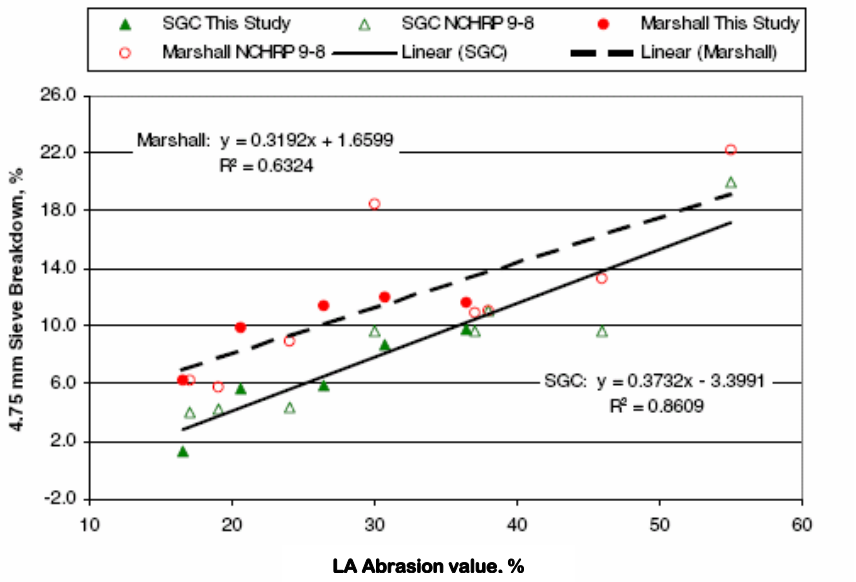

Figure 2.2: Influence of L.A. Abrasion Value on Aggregate Breakdown (after Xie and Watson 2004).

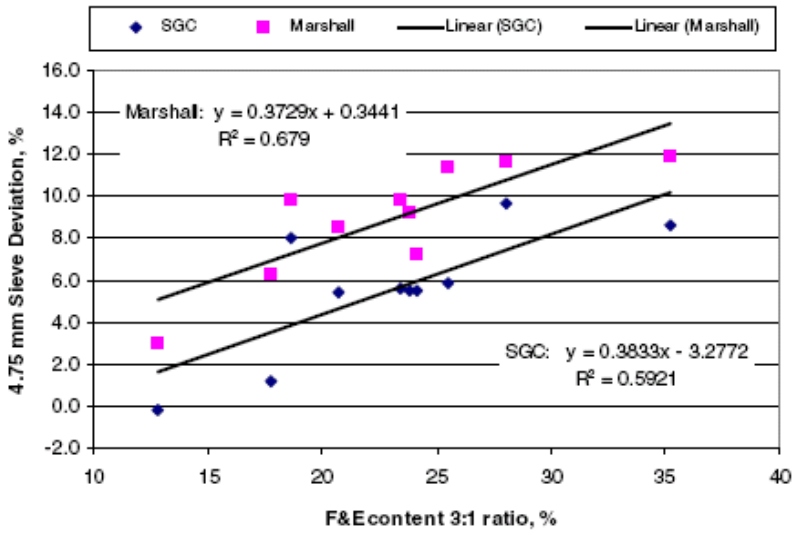

Figure 2.3: Influence of F&E Content on Aggregate Breakdown (after Xie and Watson 2004).

Methods for Characterization of Aggregates for SMA Mixtures

An important issue to address is the criteria for selecting aggregates for use in SMA such that the aggregates can resist degradation due to the high contact stresses during compaction and traffic loading. There are no well-established methods for measuring aggregate properties or for relating these properties to their performance in SMA. Therefore, several state highway agencies have specified superior aggregate properties for use in SMA, while other states require the same aggregate properties irrespective of the mix type where aggregates are used. Also, the lack of experimental methods for measuring the aggregate structure in HMA has led to limited understanding of how factors such as aggregate shape, mix design, and compaction influence the aggregate structure and, consequently, SMA performance. This lack of understanding has resulted in serious impacts on aggregate specifications as it led to the development

of design methods that tended to overemphasize the need for superior aggregate properties, rather than the development of innovative design methods to accommodate a wide range of aggregate properties.

Micro-Deval and L.A. Abrasion/Impact Tests

With the increase of aggregate contacts in SMA, more stress is applied on the coarse aggregate during compaction and traffic loading. As a result, the potential for aggregate breakdown increases compared with dense-graded mixtures. Brown and Haddock (*8*) report a strong correlation between breakdown and aggregate toughness using the L.A. abrasion test. Currently, the SMA mix design procedure listed in AASHTO MP8-01 suggests that aggregates should have a LAR maximum requirement of 30 percent.

Previous research suggested that the L.A. abrasion test may not be a sufficient method to measure aggregate quality for asphalt mixtures (*24*). The test uses a large, horizontally mounted drum that is rotated 500 times. An aggregate sample and steel spheres are placed within the drum. As the drum rotates, the aggregates and spheres are picked up and dropped with a steel plate mounted within the drum. The breakdown of aggregate is due to the severe impact loading between the steel spheres and aggregate and the abrasion of aggregates as the drum rotates. Senior and Rogers (*24*) mention that this impact loading from the steel spheres can overshadow actual breakdown due to aggregate abrasion. They also describe how hard aggregates such as granite and gneiss, which typically perform well in service, may exhibit high levels of loss in the L.A.

abrasion test due to their coarse-grained crystalline structure. On the contrary, soft aggregates may absorb the impact loads in the L.A. abrasion test and exhibit lower losses than their harder counterparts.

The Micro-Deval abrasion test follows the procedure specified in AASHTO TP58. The primary purpose of the test is to examine a coarse aggregate's ability to resist abrasion and weathering. The test induces abrasion on the coarse aggregate using the Micro-Deval machine to roll a steel jar containing the aggregate, steel spheres, and water. Prior to testing, the aggregate is saturated with water for a designated amount of time. This test is similar to the LAR (*AASHTO T96*), as they both measure the percent loss of aggregate; however, the LAR does not use water and measures impact resistance. Cooley Jr. and James (*25*) found that a poor correlation exists between LAR and the Micro-Deval test results, when compared on selected aggregates used throughout the southeastern portion of the United States. However, they did find that as L.A. abrasion results increase, so do those of the Micro-Deval test. They suggested that the poor correlation was due to the fact that each test measures different modes of degradation; the L.A. abrasion test measures impact and abrasion while the Micro-Deval measures for only abrasion.

Cooley Jr. and James analyzed 72 aggregates in the study. Each of these aggregates was characterized dependent on level of performance. They found that the mineralogy of an aggregate plays a role in its resistance to abrasion. This correlates with the findings in the study by Senior and Rogers (*24*).

Aggregate Imaging System (AIMS)

The AIMS method of capturing the characteristics of aggregates using digital imaging techniques is still relatively new. However, major steps have been taken in the development of this methodology. The aggregate imaging system provides an alternative means for the characterizing aggregates as opposed to the Superpave tests for measuring coarse aggregate shape properties, which can be laborious and time consuming (*26*).

A picture of AIMS can be seen on Figure 2.4. AIMS consists primarily of top lighting, back lighting, an auto-focus microscope, and associated software (*27, 28*). The analysis that AIMS performs to determine angularity, texture, and shape are briefly described in this paper. More details concerning this system can be found in literature (*27, 28*). Aggregate angularity is calculated using the gradient method. This method tracks the change in gradient within a particle boundary. Higher values indicate a more angular aggregate. Texture is measured using the wavelet method, in which a higher texture index indicates a rougher surface. AIMS has the ability to measure the three-dimensional shape of an aggregate. Shape is quantified using the sphericity index, which is equal to 1 for a particle with equal dimensions. The sphericity index decreases as a particle becomes more flat and elongated.

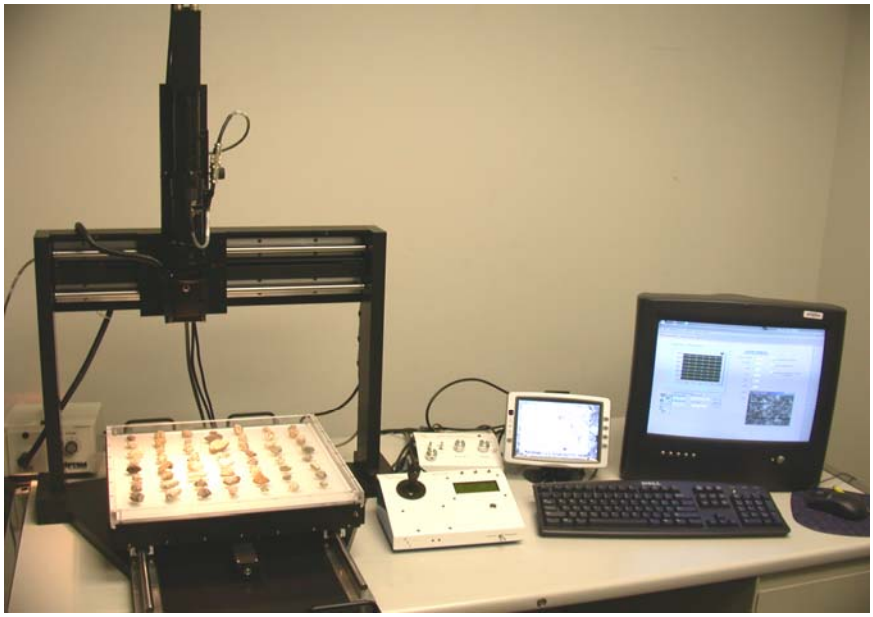

Figure 2.4: Aggregate Imaging System (AIMS).

Fletcher et al. (*26*) used AIMS to characterize fine and coarse aggregates. They found very good correlation between texture measurements and permanent deformation. Also, the AIMS measurements showed good correlation with the manual method to measure aggregate shape (flat and elongated) as shown in Figure 2.5. McGahan (*29*) also showed correlation between shape characteristics and HMA performance. A statistical analysis was performed on an aggregate database consisting of volumetric, performance, and aggregate shape measurements. The database consisted of aggregates that were used in projects funded by the Federal Highway Administration (FHWA) and the Texas Transportation Institute (TTI). The results show the there is a strong correlation between aggregate shape properties and the recorded performance of the HMA.

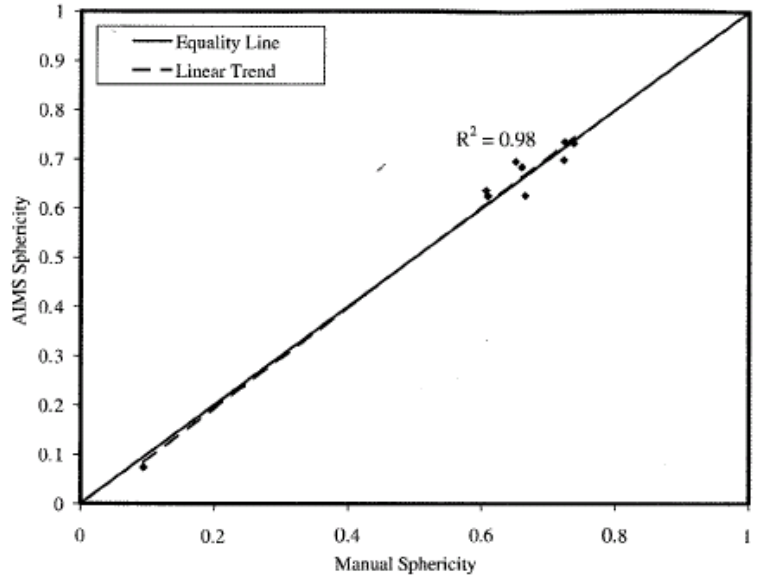

(a)

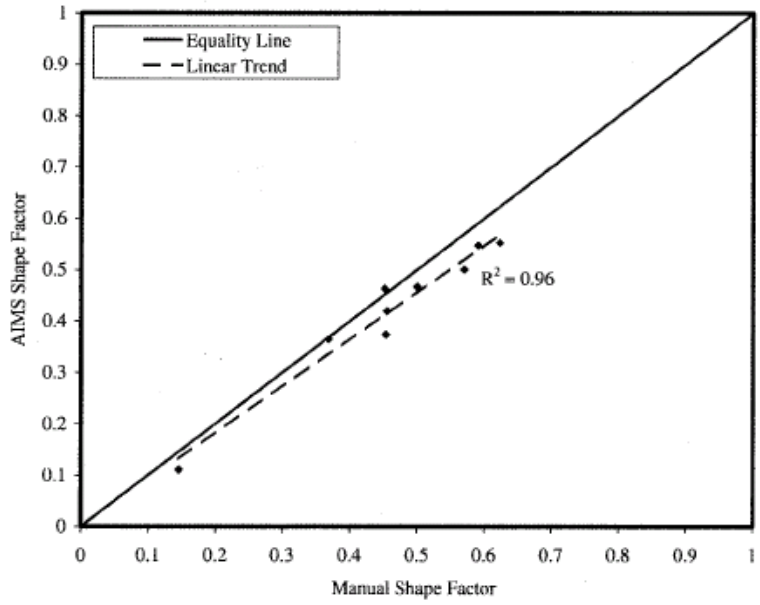

(b)

Figure 2.5: Correlation of Manual and AIMS Method for Measurement of Shape Using two Indices (a) Sphericity and (b) Shape Factor (After Fletcher et al. 2003).

A recent study at Texas A&M University led to the development of a new methodology to classify aggregates based on their shape, angularity, and texture characteristics (*27*). The study analyzed 13 coarse aggregates that represented a wide variety of aggregate type and shape characteristics. AIMS measurements showed excellent reproducibility and repeatability for the aggregates analyzed. It was also able to distinguish between the angularity and texture characteristics. For example, the study showed that some aggregates shared similar angularity; however, texture differed considerably. The findings of Al-Rousan et al. clearly support the results established by Fletcher et al. (*26*). It is important to take angularity and texture into consideration in the design of asphalt mixtures, as these studies indicate that shape characteristics correlate quite well with the performance of asphalt mixes.

X-Ray Computed Tomography

Several methodologies have been explored to determine the characteristics of aggregate in SMA. Watson et al. (*9*) explored several methods to capture the aggregate contact in open-graded friction course (OGFC) mixtures. In particular, they used the VCA method was used to determine whether the aggregate gradation achieved stone-on-stone contact once compacted. The X-ray CT was then used to verify the existence of aggregate contacts in compacted asphalt mixture specimens.

Although this study analyzed OGFC mixtures, the methodologies used are quite applicable to SMA. In particular, the VCA test to determine the existence of stone-on-stone contact is the same procedure used for SMA. The study discovered that the

designation of the breakpoint sieve played a role in whether the VCA method could determine the existence of stone-on-stone contact. The breakpoint sieve is the particular sieve that differentiates the coarse aggregate structure from the mineral filler. A guideline was suggested specifying that the breakpoint sieve should be the finest sieve size that retains at least 10 percent of the total aggregate retained.

X-ray CT was not only used to verify the VCA method but it was able to quantify the number of stone-on-stone contacts that existed in the mixtures. Watson et al. found relationships among number of contacts, compaction method, and aggregate shape characteristics.

Masad (*12*) found that the X-ray CT is a valuable tool for analyzing the internal structure of asphalt mixtures. In a recent study, Masad discussed various applications for X-ray CT. Some of these applications included determination of air void distribution and identifying stone-on-stone contacts within the asphalt mixtures.

Masad (*12*) used X-ray CT to analyze the shape characteristics of aggregates. This study involved three different aggregates: traprock, limestone, and crushed river gravel. The aggregates, which passed the 12.5 mm sieve and were retained on the 9.5 mm sieve, were put into containers that were then filled with wax to minimize disturbance of the specimen. These specimens were scanned using the X-ray CT and then analyzed to determine shape, angularity, and texture characteristics (*12*). The researchers concluded that X-ray CT is a powerful method for analyzing aggregate shape characteristics in granular materials.

Summary

SMA mixtures are designed such that applied stresses are transferred within the aggregate structure through stone-on-stone contacts. This mechanism places requirements on SMA aggregates that are different than those used in conventional dense-graded asphalt mixtures. The SMA requirements deal with the high resistance to aggregate degradation (fracture and abrasion) under applied loads. Essentially, minimization of aggregate degradation can increase rut-resistance in SMA.

The literature review in this chapter revealed that little attention has been devoted to the specifications of aggregates used in SMA. Therefore, some state highway agencies specified the use of superior aggregates without much support for these requirements, while others allowed the use of some aggregates with marginal quality in SMA.

Current SMA design methods help ensure that coarse aggregates are in contact; however, there should be more focus on characterization of aggregates that contribute to better SMA performance. Further strides need to be taken to examine other methodologies that can characterize of aggregate for SMA mixtures. This report will examine the ability of digital imaging analysis methods, X-ray computed tomography, and the Micro-Deval abrasion test to measure aggregate characteristics that affect degradation in SMA. The ability to identify methods that help characterize aggregates for use in SMA would be beneficial. The results will provide tools for measuring aggregate properties and guidelines for the selection of aggregates for SMA. Furthermore, this research would be an important to identify inferior aggregates that

should not be used in SMA or help minimize the requirements on very high quality aggregate resources that are being depleted.

CHAPTER III

EXPERIMENTAL DESIGN

Introduction

Stone matrix asphalt is a gap-graded asphalt mixture that consists of two parts: a coarse aggregate structure and a binder-rich mortar. The two components create a strong and highly rut-resistant hot mix asphalt. What makes SMA rut resistant is the stone-on-stone contact provided by the coarse aggregate structure. During the mix design of SMA it is important to ensure that the contact between the aggregate exists in order to resist deformation. NCHRP Report 425, "Designing Stone Matrix Asphalts for Rut-Resistant Pavements," reiterates the importance of this requirement for maximum SMA performance (*30*). However, the potential for degradation of the aggregates increases as the quantity of contacts increases. In this study, a number of experiments were conducted to identify aggregate characteristics and the experimental methods to measure these characteristics that pertain to an aggregate's resistance to degradation.

Materials and Mixture Design

The procedure and requirements for mix design of SMA specimens using the SGC are found in the AASHTO design standards MP8-01: Specification for Designing Stone Matrix Asphalt, and PP41-01: Practice for Designing Stone Matrix Asphalt. Mix designs for 12.5 mm SMA mixes were developed according to these specifications to handle high traffic volumes in excess of 10 million equivalent single axle loads

(ESALs). The mix design procedures demand the use of high-quality aggregate and binder based on the requirements discussed in Chapter II. Current AASHTO requirements for SMA mixture design used in this study are listed on Table 3.1.

Table 3.1: SMA Mixture Specification for SGC (AASHTO MP8-01).

Property	**Requirement**
Asphalt Content, %	6 minimum
Air Voids, %	4
VMA, %	17 minimum
VCA, %	Less than VCA_{DRC}
TSR, %	70 minimum
Draindown @ Production Temperature, %	0.30 maximum

A 12.5 mm nominal maximum aggregate size (NMAS) SMA mixture design using traprock was obtained from the Texas Department of Transportation (TxDOT). The researchers replaced the coarse aggregate fraction with other types of aggregates while maintaining the same gradation as much as possible in order to produce several mixture designs. In this study, the term "coarse aggregates" refers to particles retained on the 2.36 mm sieve. Six mixture designs were produced. The six coarse aggregates selected for use in the study are shown in Table 3.2. These aggregates exhibited wide ranges of physical characteristics. The aggregates were all sieved to each respective size and then blended to the required aggregate gradation. This helped minimize any variations in the mixture designs due to variance of blend ratios.

Table 3.2: Aggregates Used in the Study.

Mixture #	Description of Aggregate	Shape Characteristics		
		Cubical	Angular	Texture
1	Uncrushed River Gravel	H	L	L
2	Crushed Limestone 1	M	H	H
3	Crushed Glacial Gravel	H	M	M
4	Crushed Traprock	M	H	H
5	Crushed Granite	L-	M	M
6	Crushed Limestone 2	M	M	M
H: High				
M: Medium				
L: Low				
L-: Very low				

To better analyze the influence of aggregate type in the stone skeleton of SMA, the same limestone screenings and filler were used in all the mixture designs. This allows a more direct examination of SMA performance and coarse aggregate degradation by reducing variability due to differences in fine aggregates and fillers. Five percent by total aggregate weight of fly ash was used as the mineral filler in the mix designs. Also, 0.3 percent cellulose fiber by total mixture weight and 1.0 percent hydrated lime by aggregate weight were used in the mixtures. SMA mix designs require higher asphalt contents compared with conventional dense-graded mixes (*3*). With the increase of asphalt in conjunction with the gap-graded mixture, additional filler is needed to prevent draindown in SMA. Draindown can occur in an improperly designed SMA mixture where the asphalt separates and flows downward and away from the mixture, which can cause fat spots in pavements (*11*). Increased fine aggregate (minus #200), filler and cellulose fiber are used to control this occurrence (*3, 11*). Hydrated

lime is added to asphalt mixes as an anti-stripping agent to prevent the asphalt cement from separating from the aggregate in the asphalt mixture. The mix design developed by TxDOT originally used PG 76-22 asphalt, but a softer asphalt, PG 64-22, was used in this study to further emphasize the influence and interaction of coarse aggregates in SMA.

The final cumulative gradations for the six mixes are illustrated in Tables 3.3 and 3.4. As will be discussed later, these gradations were determined after the preparation of several trial mixtures with different asphalt contents. Tables 3.3 and 3.4 show the cumulative gradation of the mixture designs as well as the blend ratios of coarse aggregate, lime dry screenings, fly ash, and hydrated lime. All but one of the mix designs remained similar to the original gradations obtained from TxDOT for the traprock mixture. However, during the initial mix design process, the gradation obtained from the TxDOT gradation deemed suitable for the traprock, limestone 2, and granite aggregate mixtures. The fine aggregate portion of the gradation for the crushed glacial gravel was slightly altered in order to meet specifications, which can be seen in Table 3.4.

Minor revisions were made to three aggregate types (glacial gravel, river gravel, and limestone 1). In the crushed glacial gravel the fly ash was lowered to 4 percent, increasing the amount of air voids in the compacted mixture, which then enabled the

Table 3.3: SMA Gradation for River Gravel, Granite, Limestone 1, Limestone 2, and Traprock.

Sieve Size (in)	Sieve Size (mm)	% Passing				
		Cumulative Gradation	Coarse Aggregate	Dry Screenings	Mineral Filler (Fly Ash, 4.0%)	Hydrated Lime, (1.0%)
3/4"	19.00	100	100	100	100	100
1/2"	12.50	89.30	89.30	100	100	100
3/8"	9.50	59.90	59.90	100	100	100
#4	4.75	27.77	27.77	100	100	100
#8	2.36	17.92	17.92	100	100	100
#16	1.18	15.11	0	15.11	100	100
#30	0.60	12.30	0	12.30	100	100
#50	0.30	10.71	0	5.99	94.50	100
#100	0.15	9.86	0	5.34	90.25	100
#200	0.075	9.00	0	4.70	86.00	100
Pan	0	0	0	0	0	0

Table 3.4: SMA Gradation for Crushed Glacial Gravel.

Sieve Size (in)	Sieve Size (mm)	% Passing				
		Cumulative Gradation	Coarse Aggregate	Dry Screenings	Mineral Filler (Fly Ash, 4.0%)	**Hydrated Lime, (1.0%)
3/4"	19.00	100	100	100	100	100
1/2"	12.50	89.30	89.30	100	100	100
3/8"	9.50	59.90	59.90	100	100	100
#4	4.75	27.77	27.77	100	100	100
#8	2.36	17.92	17.92	100	100	100
#16	1.18	14.11	0	14.11	100	100
#30	0.60	11.30	0	11.30	100	100
#50	0.30	9.71	0	5.93	94.50	100
#100	0.15	8.86	0	5.25	90.25	100
#200	0.075	8.00	0	4.56	86.00	100
Pan	0	0	0	0	0	0

mixture to meet specifications. With several revisions to the gradation of the river gravel mixture, it was later decided that the original mixture design met closest to the

mixture design specification. Three sets of mixture designs were made for the limestone 1 aggregate. The three mixture designs involved adjustments from lowering the mineral filler to adjusting the gradation of the coarse aggregate structure. Ultimately, the original mixture design for the limestone 1 met closest to specifications. Illustrations of the final gradations can be seen on Figure 3.1. This figure illustrates how the final gradations for the six aggregates are relatively the same with exception the glacial gravel mixture, which is a bit coarser that to the other mixtures.

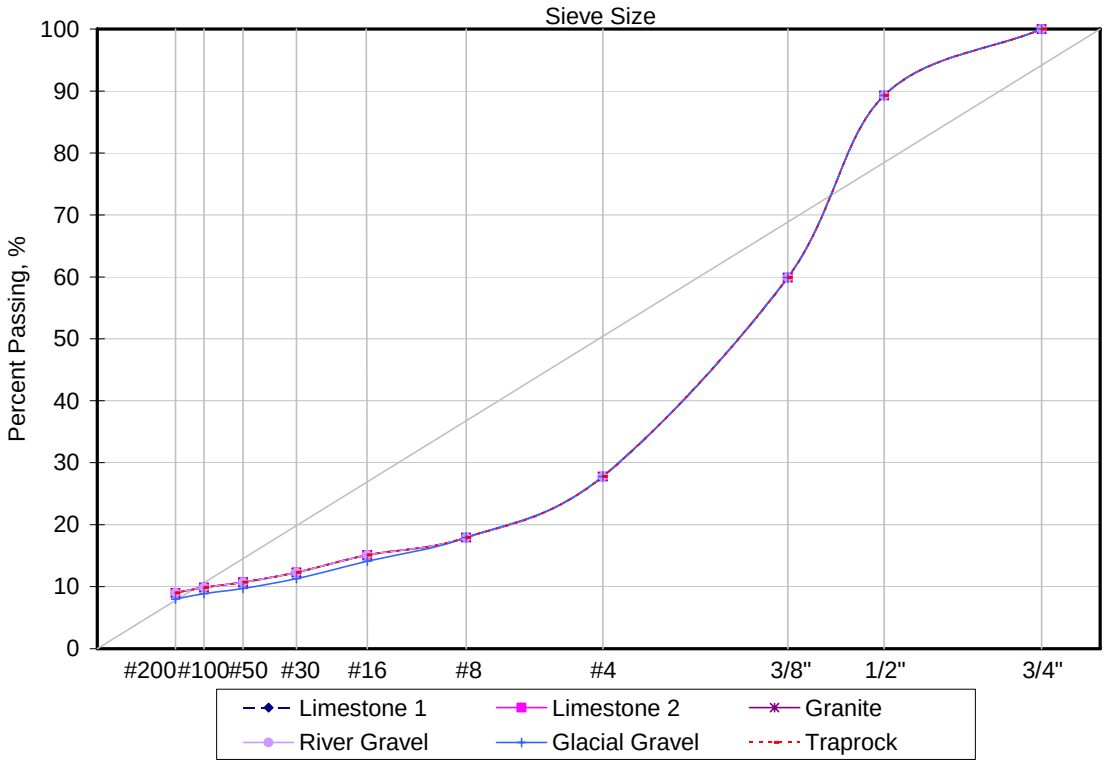

Figure 3.1: Mixture Design Gradations.

Bulk specific gravities of the compacted specimens were determined using the CoreLok® vacuum sealing device. SMA specimens have very large voids on the surface

of the compacted specimens (*5*). Xie and Watson (*5*) recommended that for coarser SMA mixes (i.e., 12.5 mm and larger), the CoreLok® had less potential for error as opposed to the SSD method. Therefore, it was decided that the CoreLok® was best suited for this particular application. The procedure for using the CoreLok® is according to ASTM D6752 and D6857.

Studies conducted by Brown and Brown and Haddock. specify the importance of ensuring that no more than 30 percent of total aggregate weight passes the #4 sieve (*1, 8*). The VCA_{DRC} method was used according to AASHTO T19 to evaluate the stone-on-stone contacts in all mixtures. The VCA of the mix and the VCA of the coarse aggregate were then compared to ensure that the mix would achieve stone-on-stone contact when compacted using the method.

Specimen Preparation

The SMA specimens were prepared using the specifications listed in the AASHTO provisional standards MP8-01 and PP41-01. The SGC was used to prepare all specimens used in this study. The mixes were compacted using molds that were 6 inches in diameter; specimen heights were dependent on the tests conducted on the specimens. Compaction heights for the asphalt specimens for the flow number test were 7 inches, while specimens prepared for the aggregate imaging analysis were compacted to approximately 4.5 inches.

In the laboratory, initial batches of 12,700 grams of aggregate were made in preparation for the mix design procedure. For each coarse aggregate type, three initial

batches were prepared to have 5.0 percent, 5.5 percent and 6.0 percent asphalt content. Each batch yielded two 6 inch diameter, 4,500 gram specimens, and two 1,500 gram Rice density specimens. Asphalt mixtures were weighed and compacted using the SGC to 100 gyrations. After compaction, the specimens were allowed to cool and the bulk and maximum theoretical specific gravites were obtained using the CoreLok® vacuum sealing device and Rice density apparatus, respectively. The percent air voids was calculated and plotted versus asphalt content. This allowed for the optimum asphalt content at 4 percent air voids to be obtained.

If the three batches did not include the required 4 percent air voids in the total mix after compaction, additional batches with different asphalt contents were prepared until the target air void content was achieved. For example, Figure 3.2 illustrates the air void content plotted versus the asphalt content for traprock, where four batches were prepared in order to determine the asphalt content at 4 percent air voids.

Additional specimens were prepared for asphalt extraction using the ignition oven and mechanical sieve analysis of the remaining aggregates of SMA specimens before and after compaction in the SGC. Asphalt specimens of 2,200 grams were used during the sieve analysis testing, which follows the recommendations of sample size specified for 12.5 mm mixtures in AASHTO T30.

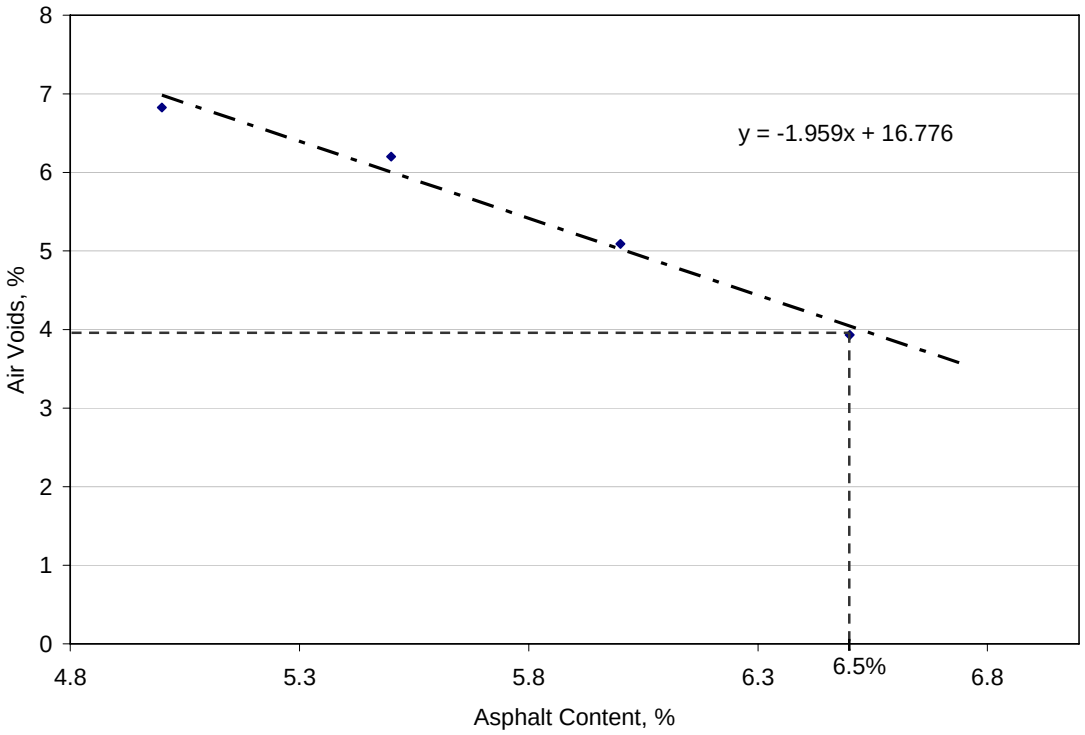

Figure 3.2: Determination of Optimum Asphalt Content for Traprock.

The specimens used for X-ray CT analysis were prepared using 4,600 gram aggregate samples and were later mixed with the optimum asphalt content obtained during the mix design process. Four samples were prepared for each of the six mixture designs. Two of these four samples were compacted to 100 gyrations, while the other two specimens were compacted to 250 gyrations. This high number of gyrations was used to induce aggregate breakdown. Dessouky et al. (*22*) found that volumetric change in a specimen decreases significantly after about 100 gyrations. They also suggested that specimens experience shear stresses among aggregate particles between 100 and 250 gyrations. It was not practical to compact specimens to more than 250 gyrations since

specimens cooled and stiffened, making it harder to apply the compaction forces (vertical pressure and angle of gyration) in the SGC.

Specimens prepared for the flow number test were compacted using the SGC into 6 inch diameter specimens that were 7 inches tall. Two specimens were prepared from each mix for the flow number test. These specimens were then cored to a diameter of 4 inches and trimmed to a height of 6 inches. Trial specimens were created to establish a correlation between the air void content of the compacted specimen and the air void content of the cored specimens. The amount of asphalt mix added to each mold for compaction varied for each mix design in order to achieve 7 percent air void content after the sample was trimmed. An example of the trimmed specimen used in the flow number test is illustrated in Figure 3.3.

Table 3.5 includes a summary of the specimens prepared for each of the mix tests conducted in this study. The data from the mix design process are listed in Table 3.6. In conjunction with the SMA requirements in Table 3.3, the six mix designs either met or came close to passing specifications.

Table 3.5: Summary of Specimens Prepared.

Test	Number of Specimens	Specimen Size
Extraction and Mechanical Sieving	2, 100 gyrations	2,200 grams
	2, 250 gyrations	
	2, non-compacted	
X-Ray CT	4, 100 gyrations	4.5" x 6" Dia.
	4, 250 gyrations	
Flow Number	2, 7% Air Voids	6" x 4" Dia.

Figure 3.3: Example of Trimmed Specimen for Flow Number Test (Glacial Gravel).

Table 3.6: Mix Design Results.

Aggregate Source	Aggregate Bulk Sp. Gravity	Asphalt Content	VMA
River Gravel	2.617	5.5	14.00
Limestone 1	2.655	5.0	14.64
Glacial Gravel	2.637	6.0	16.26
Traprock	2.966	6.5	19.71
Granite	2.621	7.5	19.25
Limestone 2	2.652	5.3	14.00

Resistance to Abrasion Using the Micro-Deval Test and Imaging Techniques

Degradation of Coarse Aggregate by Micro-Deval Abrasion

In SMA, it is important to examine physical characteristics of the aggregates and their behavior when abrasion is induced. Several methods were used in the literature to examine the physical characteristics of aggregates under an abrasive load. Typically, SMA mixture design requires the use of the L.A. abrasion test to determine the abrasion resistance of aggregate (*7, 8*). However, recently the Micro-Deval test has gained popularity as a reliable method for measuring aggregate abrasion; hence, this test was used to determine aggregate toughness for the six coarse aggregates.

The Micro-Deval abrasion test follows the procedure specified in AASHTO TP58. The primary purpose of the test is to examine a coarse aggregate's ability to resist abrasion and weathering. The test induces abrasion on the coarse aggregate by rolling a steel jar that contains the aggregate, steel spheres, and water. The test requires a 1,500 gram aggregate sample that consists of aggregate passing the 12.5 mm sieve and retained on the 9.5 mm (3/8 inche), 6.3 mm (1/4 inch), and 4.75 mm (#4) sieves. Approximately 750 grams should be retained on the 9.5 mm sieve, 375 grams on the 6.3 mm sieve, and 375 grams on the 4.75 mm sieve. Prior to testing, the aggregate is saturated with water for at least 1 hour. Once saturation is complete, the sample is placed in the Micro-Deval container with approximately 5,000 grams of stainless-steel spheres, and water. The contained is placed in the machine and then rotated at 100 rpm for approximately 105 minutes. Once the machine is turned off, the aggregate is carefully rinsed while removing the steel spheres, and then oven dried. The material passing the 1.18 mm

(#16) sieve is also discarded. Once the sample is dry, the weight is recorded and the percent loss is calculated. This test is similar to the L.A. abrasion test (*AASHTO T96*), as they measures the percent loss of the aggregate; however, the L.A. abrasion test does not use water and the Micro-Deval abrasion test does not account for impact resistance.

Measurement of Aggregate Shape Characteristics using AIMS

It is important to realize that aggregate shape characteristics also play a major role in the performance of asphalt concrete. Recent advancements in understanding aggregate shape characterization have led to a new methodology to classify aggregate characteristics (*AASHTO 2001*). This methodology utilizes the AIMS to directly measure and analyze aggregate characteristics such as texture, sphericity, and angularity. The analysis is statistically based, as AIMS measures a distribution of aggregate characteristics from an assortment of sources and sizes. The description of AIMS is given in Chapter II, while more details can be found in the literature from Al-Rousan et al. and Masad (*27, 28*).

For this study, AIMS was used to measure the angularity, texture, and shape of coarse aggregates before and after the Micro-Deval test in order to compute the change in physical characteristics of the aggregates due to the induced abrasion. The focus of the analysis was pertained to the aggregate retained on the 9.5 mm (3/8 inch) and 4.75 mm (#4) sieves. The coarse aggregates were initially sieved according to the sieves specified in the TxDOT gradation that is used in this study. The samples were randomly selected for each of the aggregate sources. AIMS was then used to measure the shape

characteristics of the random sample. A macro routine developed by Dr. Masad of Texas A&M University was used to determine the average shape properties for the coarse aggregate based on the representative gradation used in this study. This was used to obtain the average results of AIMS for both before and after the Micro-Deval test. An illustration of the macro results is show on Figure 3.4.

Sieve Size	Percent Passing	Angularity-Gradient Method	Angularity-Radius Method	Form 2-D	Sphericity	Texture
1 1/2 inch (37.5 mm)	100.00	2837.98	10.34	7.28	0.67	278.88
1 inch (25.0 mm)	100.00	2837.98	10.34	7.28	0.67	278.88
3/4 inch (19.0 mm)	100.00	2837.98	10.34	7.28	0.67	278.88
1/2 inch (12.5 mm)	89.30	2837.98	10.34	7.28	0.67	278.88
3/8 inch (9.5 mm)	59.90	2837.98	10.34	7.28	0.67	278.88
#4 (4.75 mm)	27.77	2189.03	12.04	9.73	0.55	251.84
#8 (2.36 mm)	17.92	2189.03	12.04	9.73		
#16 (1.18 mm)	15.11	2189.03	12.04	9.73		
#30 (0.6 mm)	12.30	2189.03	12.04	9.73		
#50 (0.3 mm)	10.71	2189.03	12.04	9.73		
#100 (0.15 mm)	9.86	2189.03	12.04	9.73		
#200 (0.075 mm)	9.00	2189.03	12.04	9.73		

	Average Shape Properties		
	All Blend	Coarse	Fine
Angularity-Gradient Method	2260.77	2465.74	2189.03
Angularity-Radius Method	11.85	11.32	12.04
Form 2-D	9.46	8.69	9.73
Sphericity		0.58	
Texture		263.37	

Figure 3.4: Macro Used for AIMS Results.

Aggregate Degradation Due to Compaction

Mixture Stability during Compaction Using Contact Energy Index

The CEI is a stability index for HMA mixes that are compacted in the SGC. The CEI indicates the ability of a mix to develop aggregate contacts and resist shear deformation (*22*) and is dependent on the summation of applied stresses and induced deformation during compaction of a specimen. Application of this method uses the compaction data obtained from the SGC (*21*). A Microsoft Excel® macro developed by Dessouky et al. enables a user to input data from the SGC and yields the appropriate CEI value for that particular mix. For this study, the six mixtures developed, each yielding four specimens, were compacted to 250 gyrations. These specimens were later used for the X-ray CT and sieve analyses. Once the data were collected, they were entered into the macro program, and the average CEI of each mix was recorded.

Mechanical Sieve Analysis of Compacted Specimens

Because the performance of SMA is dependent on the aggregate quality and stone-on-stone contact, the breakdown of aggregate during compaction was also examined. In this study, the asphalt specimens were compacted using the Superpave gyratory compactor. For each of the six mix designs, two specimens were compacted to 100 gyrations and two specimens were compacted to 250 gyrations. The 100 gyration specimens had a target air void level of 4 percent. The specimens were compacted to 250 gyrations in order to induce aggregate breakdown.

The ignition oven was used to extract the asphalt and provide a clean aggregate sample. The clean aggregate samples were subjected to sieve analysis to compare the gradations of the pair of 100 gyration samples with the gradations of the 250 gyration

samples. Two replicate samples were analyzed in order to track the consistency of the results. Clean aggregate from non-compacted mixtures that were put into the ignition oven were compared. These non-compacted mixtures served as a control to determine any changes in gradation due to the exposure to the extreme heat of the ignition oven. This comparison showed aggregate breakdown due to compaction at 100 versus 250 gyrations.

Ignition oven extraction followed the procedure specified in AASHTO T30. The purpose of the test is to perform a mechanical sieve analysis on the SMA mixes before and after to compaction. This allows determination of whether crushing occurred in the SMA specimens during compaction. The tests consist of a total of six specimens for each mixture design. As will be shown in the following chapter, all of the samples tested had excellent consistency between replicates; thus, their averages were taken for the results. In addition, all the specimens were properly mixed according to the mix designs established in this study.

Aggregate Imaging Analysis Using X-Ray Computed Tomography

The X-ray CT is a nondestructive technique that captures the internal structures of an asphalt mix. It is a helpful tool to analyze the internal structural packing, which can be a useful tool to analyze SMA specimens since they rely on stone-on-stone contact. Previous studies have been able to utilize X-ray CT imaging to obtain surface area and percent air voids and determine air void connectivity in asphalt specimens (*12, 31 – 33)*. X-ray CT can be a helpful tool to analyze the internal structural packing,

stone-on-stone contacts, and breakage of particles. For this analysis, an additional two specimens were compacted to 100 gyrations and another two were compacted to 250 gyrations for each mix design. The specimens were then scanned with the X-ray CT at 1 mm incremental depths. An example of an image taken by the X-Ray CT is illustrated in Figure 3.5. X-ray CT images from a total of 28 specimens were taken. The total number of specimens is representative of the six aggregate types used in the study.

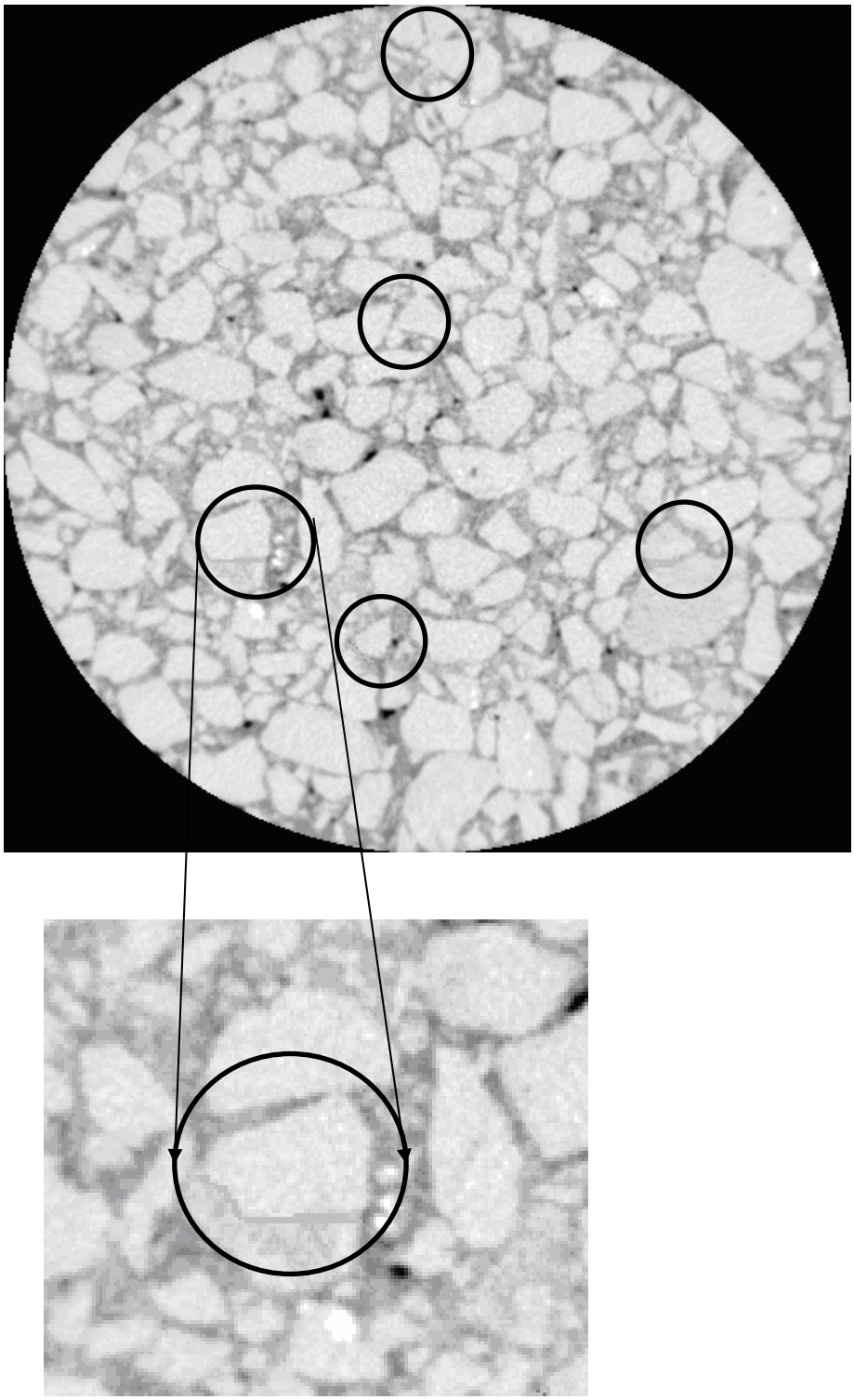

Figure 3.5: X-Ray Image of Limestone 1 at 250 Gyrations with Circles Highlighting Areas with Crushed Particles.

The focus of X-ray CT imaging, was to analyze the internal structures of the SMA specimens that were compacted to 4% air voids and compare them to the 250 gyration specimens. The software program Image Pro® was used to analyze of the X-ray images. A macro was developed to analyze the size distribution of particles in X-ray CT images. In this macro, the method developed by Tashman et al. (*34*) was used to separate particles. This method converts grayscale images to black-and-white images and an additional filter is applied to separate the particles. Essentially, a threshold value was needed during the black-and-white conversion of the images. This value was obtained for each mixture design prior to filtering. The threshold determined the level of filtering of the grayscale image into a black-and-white image and was dependent on the grayscale value that distinguished the coarse aggregates from the mortar. This filtering enables Image Pro® to distinguish the difference between the aggregate and mortar in the image. The image color is introverted, and a "thinning" filter is applied to show the edges of the aggregates selected. Once selected, a separation filter is applied to separate aggregates that are in contact. This filter is dependent on the elongation and angularity of a selected aggregate. Based on any breaks in the elongation or angularity of an aggregate, the macro selects the aggregate based on this criterion and splits the selected object.

The median (50^{th} percentile), 25^{th}, and 75^{th} percentiles of the weight retained on each sieve size among all images were calculated, and the difference in the three percentiles between specimens compacted at 100 gyrations and 250 gyrations was then determined. The macro used in the analysis focused on the aggregates retained on the

12.5 mm (½ inch) to the 4.75 mm (#4) retained portion of the gradation, as this portion is the bulk of the gradation. Image Pro® was then used to determine the extent of aggregate breakdown in the 250 gyration specimens compared to the specimens gyrated to 100 gyrations.

Aggregate Degradation Due to Repeated Dynamic Loading

The primary purpose of the flow number test was to induce aggregate crushing resulting from loading. The flow number test captures fundamental material properties of an HMA mixture that correlate with rutting performance (*35*). In this test procedure, axial dynamic compressive stress is applied in a haversine waveform with a wavelength of 0.1 seconds followed by a rest period of 0.9 seconds on cylindrical HMA specimens until tertiary deformation is observed. The number of load repetitions to cause tertiary permanent deformation is termed as flow number. The primary purpose of the flow number test in this project was to induce aggregate crushing resulting from repeated dynamic loading.

This test was conducted following the procedure suggested by NCHRP Project 9-19 (*35*). In this project, all mixtures were tested at 37.8° C and 310 kPa. Relatively lower temperature and higher stress were selected in order to induce permanent deformation caused primarily by aggregate degradation. Specimens were tested at an ambient temperature of 100° F, and a 45 psi load was applied with 0.1 second loading times and 0.9 second resting periods. Specimens were prepared using a six inch diameter mold and were compacted to a height of 7 inches. The amount of mix put into

the mold was varied in order to obtain 7 percent air voids in the specimens after they were trimmed to size. The final size prior to testing was a four inch diameter specimen with a height of 6 inches.

Aggregates were extracted from the specimens using the ignition oven after the flow number tests. Sieve analysis was performed on the recovered aggregates. Aggregate gradations after the flow number test were compared to the gradations of control samples that were not tested with flow number test.

Summary

This chapter discussed the materials used in this study, and the mix design procedures used to design SMA mixtures and prepare specimens. The SMA gradation obtained from TxDOT applied to all of the aggregates with a few minor changes that ensured that specifications for SMA were closely met. In addition, other changes were made to minimize any possible variations in data due to asphalt binder type, fillers, and other extraneous factors.

Several test methods to characterize degradation of coarse aggregates in SMA were presented in this chapter. Specifically, the test methods were selected to describe different forms of degradation in SMA. These forms include degradation of coarse aggregate by abrasion, which was studied using AIMS and the Micro-Deval test, degradation due to compaction by means of the SGC followed by mechanical sieve analysis, and aggregate degradation due to dynamic loading through the use of the flow number test followed by mechanical sieve analysis.

CHAPTER IV
RESULTS AND DATA ANALYSIS

Introduction

This chapter presents the results of the experimental measurements discussed in chapter III. These results include aggregate degradation due to compaction, change in aggregate structure stability during compaction, aggregate degradation under repeated loading, aggregate weight loss due to abrasion in the Micro-Deval, and change in aggregate shape characteristics after abrasion. The chapter discusses the relationships amoung these results and concludes with guidelines on assessing the suitability of the use of aggregates in SMA resistance to abrasion using the Micro-Deval test and imaging techniques.

Aggregate Degradation Due to Micro-Deval Abrasion Test

Results of the Micro-Deval test are listed in Table 4.1. These results are the average of two tests. The percentage in this table represents the aggregate weight loss passing the 1.18 mm (#16). Previous research indicates that aggregates used for premium surfaces such as SMA would have a weight loss no higher than 15 percent (*36*). Limestone 2 experienced the highest percent loss (23.5 percent), while uncrushed river gravel experienced the lowest percent loss (4.6 percent). Table 4.1 illustrates that all of the aggregate types used in the study are below the maximum Micro-Deval loss of 15 percent for high-traffic pavement as specified by Lane et al. (*36*), with the exception

of limestone 2 which exhibits 23.5 percent loss. Results of the individual tests are provided in Appendix A1.

Table 4.1: Results for Degradation of Coarse Aggregate via Micro-Deval Abrasion.

Mixture #	Description	Micro-Deval Loss (%)
1	Uncrushed River Gravel	4.6
2	Limestone 1	12.6
3	Crushed Glacial Gravel	11.2
4	Traprock	11.3
5	Granite	5.6
6	Limestone 2	23.5

AIMS was used to measure the angularity, texture, and shape of coarse aggregates before and after the Micro-Deval test in order to compute the change in physical characteristics of the aggregates due to abrasion. The values were then used to obtain the average shape characteristics for each of the mixture designs. These results are shown in Figure 4.1. In this figure, the percent change is defined as difference in an aggregate characteristic before and after the Micro-Deval test divided by the shape index before Micro-Deval test. The figures and details of the shape characteristic values calculated from the AIMS analysis can be found in the Appendix.

The percentages represented in Figure 4.1 are useful for describing how the aggregate characteristics have changed. Figure 4.1a shows changes in angularity. A negative change in angularity indicates that an aggregate became less angular after the Micro-Deval test. Figure 4.1b shows changes in aggregate sphericity, where more

elongation of aggregate after Micro-Deval is represented by the negative change. In Figure 1c, negative changes mean that an aggregate lost some of its texture, and positive changes are indicative of increase in aggregate roughness.

The general trends illustrated in the figures show that after the Micro-Deval test most of the aggregates became more polished and less angular. The uncrushed river gravel increased in elongation and angularity after the Micro-Deval test. This finding suggests that the Micro-Deval test caused some breakage in this aggregate leading, to an increase in angularity (Figure 1a). The glacial gravel, however, experienced a 30 percent reduction in angularity due to abrasion.

After the Micro-Deval test, four of the six aggregates became more elongated, which is denoted by the negative percent change in Figure 4.1b. Also in this figure, Limestone 1 exhibited a 70 percent increase in elongation of particles indicating that particles experienced breakage. Granite and the river gravel exhibited less than 10 percent change in sphericity. However, the glacial gravel and limestone 2 experienced an increase in sphericity, most likely due to abrasion of the sharp corners at the surface of these particles. Figure 4.1c shows that four of the six aggregates became more polished. Limestone 1 experienced the most change compared to the other four aggregates. The texture results indicate that the river gravel exhibited a little increase in texture. This could be due to the exposure of new textured surfaces when aggregates were crushed. The increase in texture of the granite could indicate that the abrasion in the Micro-Deval exposed surfaces with even more texture.

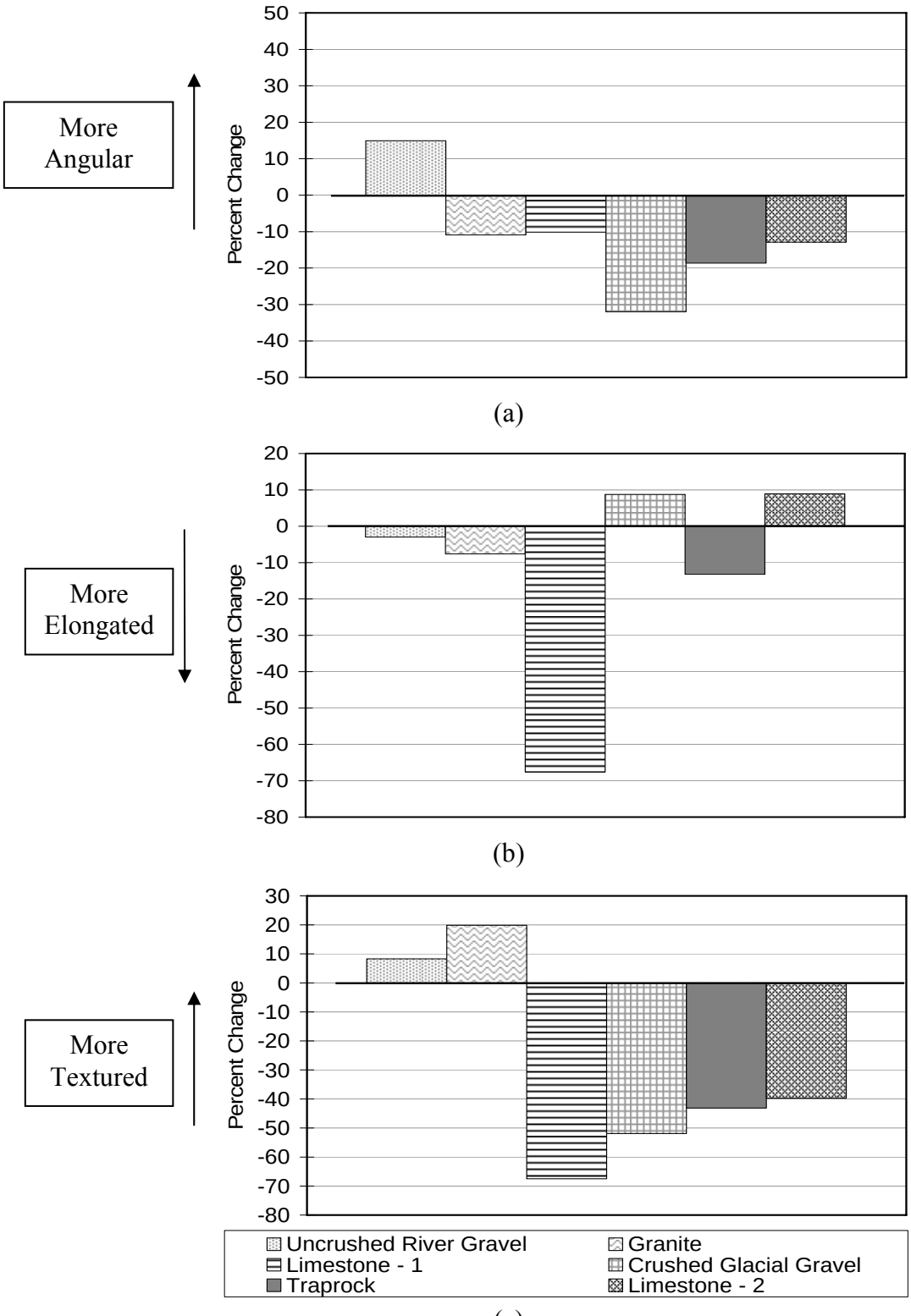

Figure 4.1: Results of AIMS Analysis for (a) Angularity (b) Sphericity (c) Texture.

Aggregate Degradation Due to Compaction

Mechanical Aggregate Size Analysis

Very good repeatability was obtained from the analysis of aggregate gradations of replicates as evident in the example of gradation analysis shown in Figure 4.2. This figure illustrates the results of the gradations with respect to the percent passing each particular sieve. The gradations of the specimens compacted to 100 and 250 gyrations are plotted versus the design gradation as well as the gradation of specimens that were mixed but not compacted. The figure shows that the non-compacted mixtures do not differ much from the original gradations, implying that the ignition oven did not have a significant effect on the gradation of the samples. The slight differences between the original and non-compacted specimens are attributed to experimental errors in sampling and weighing of aggregates or breakdown that may have occurred during the extraction process. Details of sieve analysis results can be found in Appendix A2.

Figures 4.2 to 4.7 show that aggregate breakdown did occur due to compaction. Breakdown is apparent within the first 100 gyrations of compaction with all mixtures; however the severity of breakdown varies. Glacial gravel exhibits a similar trend to limestone 2, where there is a small difference between the 100 gyration and 250 gyration curves as shown in Figure 4.2 and 4.7, respectively. The 12.5 mm (1/2 inch) sieve did not show a significant change in gradation; however, the gradations did become finer from the 9.5 mm (3/8 inch) sieve and smaller sieves.

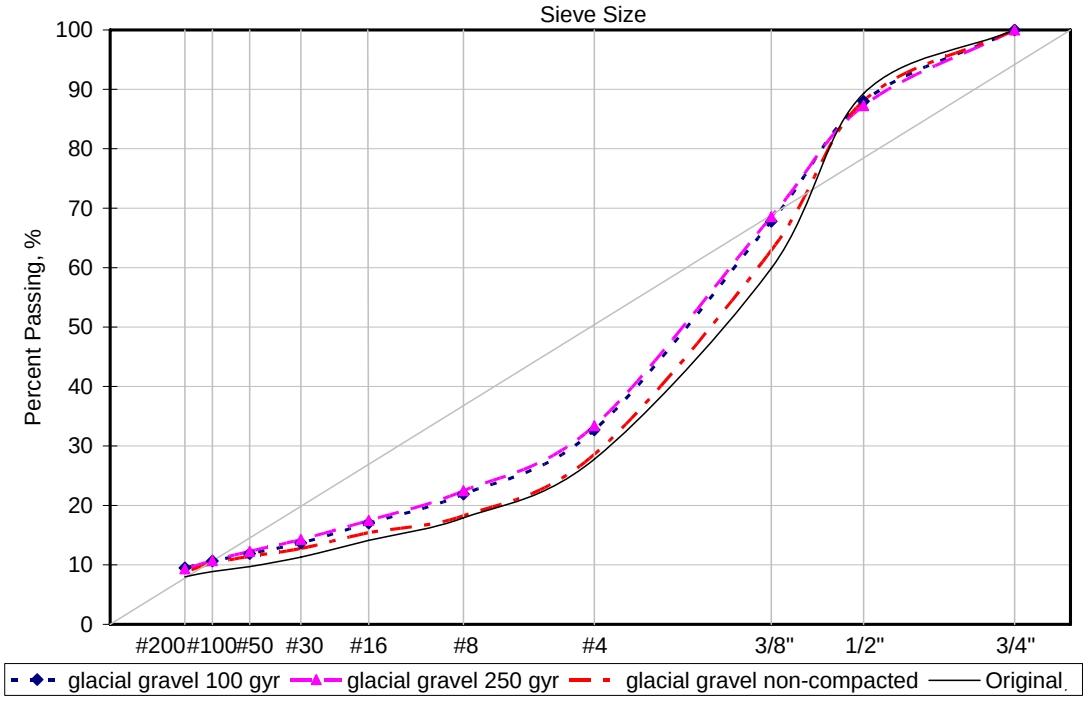

Figure 4.2: Sieve Analysis Results for Glacial Gravel.

Traprock showed minor change in gradation with the exception of the amount passing the 12.5 mm (1/2 inch) sieve as shown on Figure 4.3. The aggregate retained on the 9.5 mm (3/8 inch) sieve showed an increase of approximately 10 percent. Figure 4.3 also illustrates that the gradation of the samples compacted increased slightly when compared to the non-compacted specimen. The results suggest that any breakdown that occurred in the samples was distributed throughout the smaller sieves.

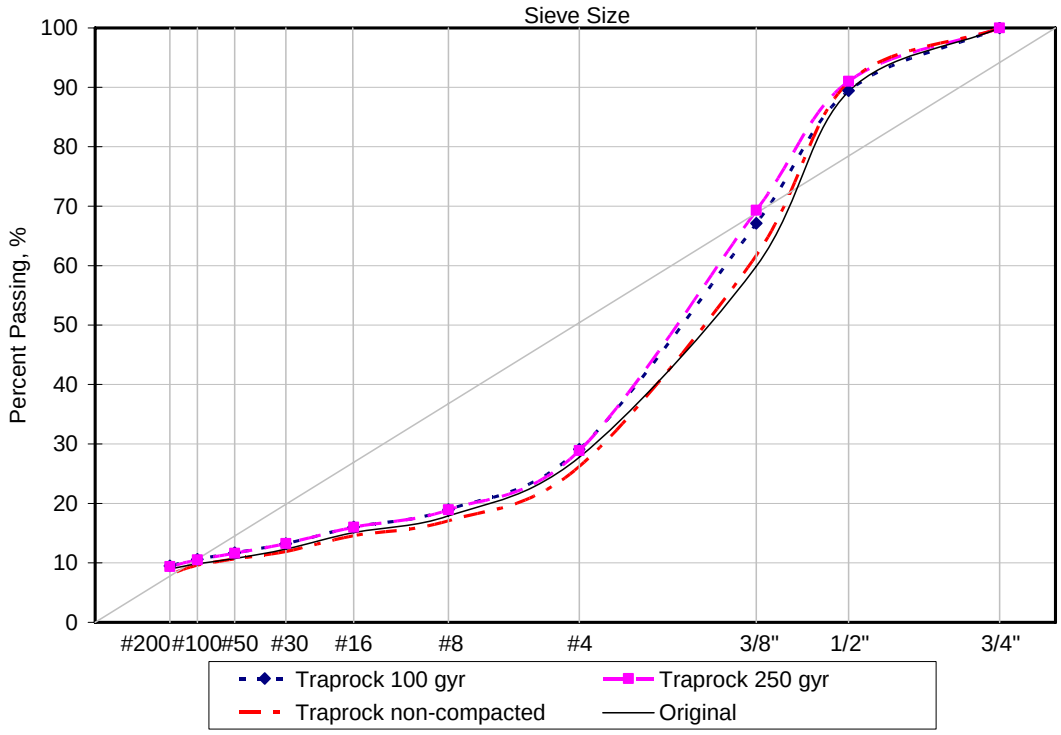

Figure 4.3: Sieve Analysis Results for Traprock.

Figure 4.4 shows that limestone 1 exhibited a significant change in gradation when compacted to 250 gyrations. Breakdown due to the sample being compacted to 100 gyrations caused an increase of approximately 3 percent in the amount of material passing the sieves. This particular aggregate showed a significant change in the amount of breakdown that occurred between 100 gyrations and 250 gyrations. The other aggregates illustrate minor changes when sample are compacted from 100 to 250 gyrations. In this particular case, Figure 4.4 shows that the amount passing each respective sieve after 250 gyrations increased by approximately 2 percent from the results shown for the 100 gyration specimen.

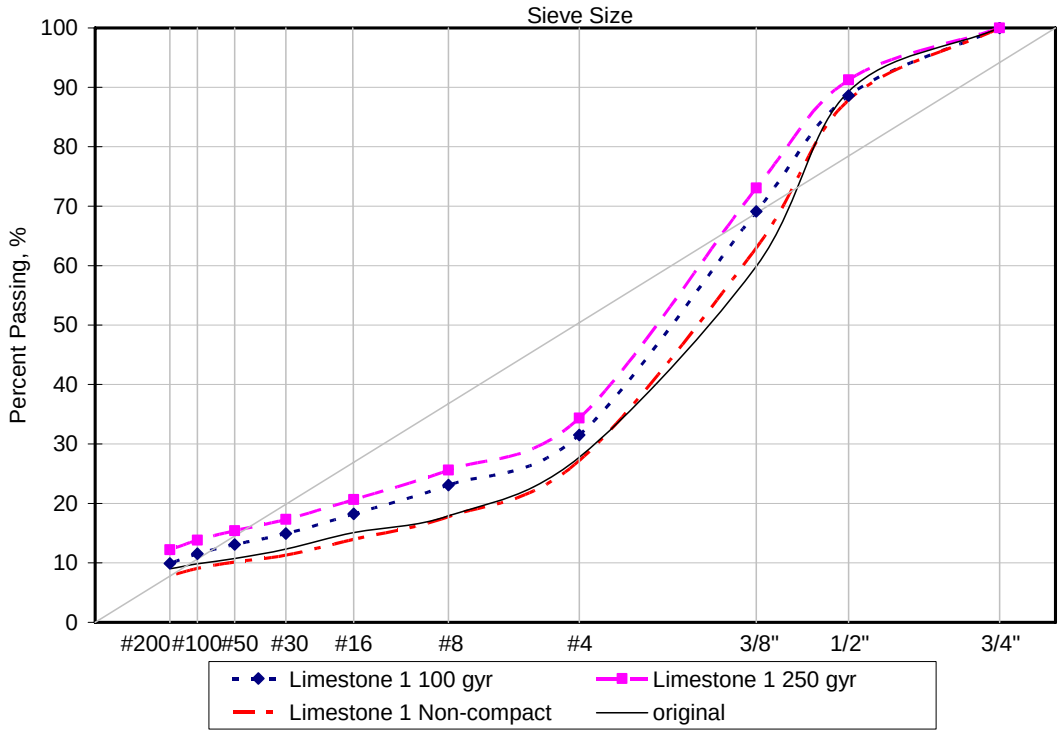

Figure 4.4: Sieve Analysis Results for Limestone 1.

Limestone 2, shown on Figure 4.5, showed no major changes between the specimens compacted to 100 gyrations and 250 gyrations. It appears that this mixture experienced maximum aggregate breakdown when compacted to 100 gyrations. The specimens did show a significant increase over the original and noncompacted specimens in the percent passing each respective sieve. The 12.5 mm (1/2 inch) sieve showed no apparent changes in gradation as opposed to the smaller sieve. The results suggest that extreme breakdown may have occurred throughout the aggregate structure when compacted.

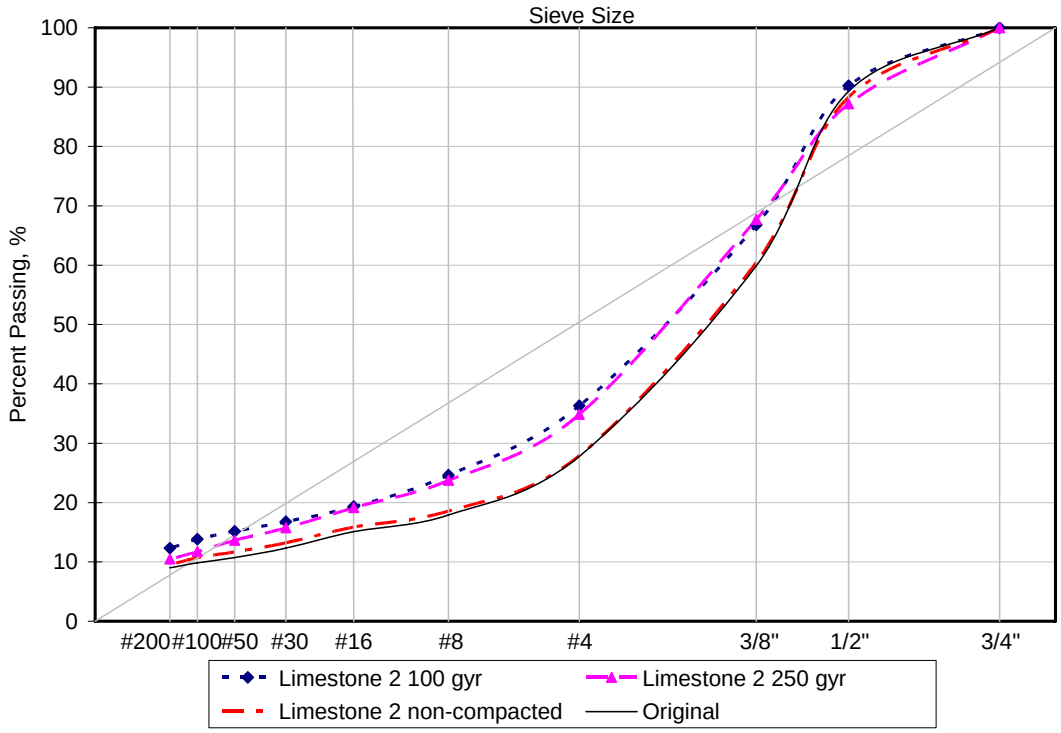

Figure 4.5: Sieve Analysis Results for Limestone 2.

Figure 4.6 shows that granite exhibited a small amount of breakdown compared to the other mixtures. When the compacted specimens were compared to the non-compacted specimen, breakdown was observed on sieves larger than the 2.38 mm (#8) sieve, but none of the smaller sieves showed significant increased changes in gradation. Gradations did not change when samples were exposed to increased numbers of gyrations. The uncrushed river gravel also exhibited minor aggregate breakdown as shown on Figure 4.7. Breakdown was slightly more significant when compared to the results of the granite as shown on Figure 4.6. There is an increase in the aggregates passing the sieves smaller than 12.5 mm (1/2 inch) sieve.

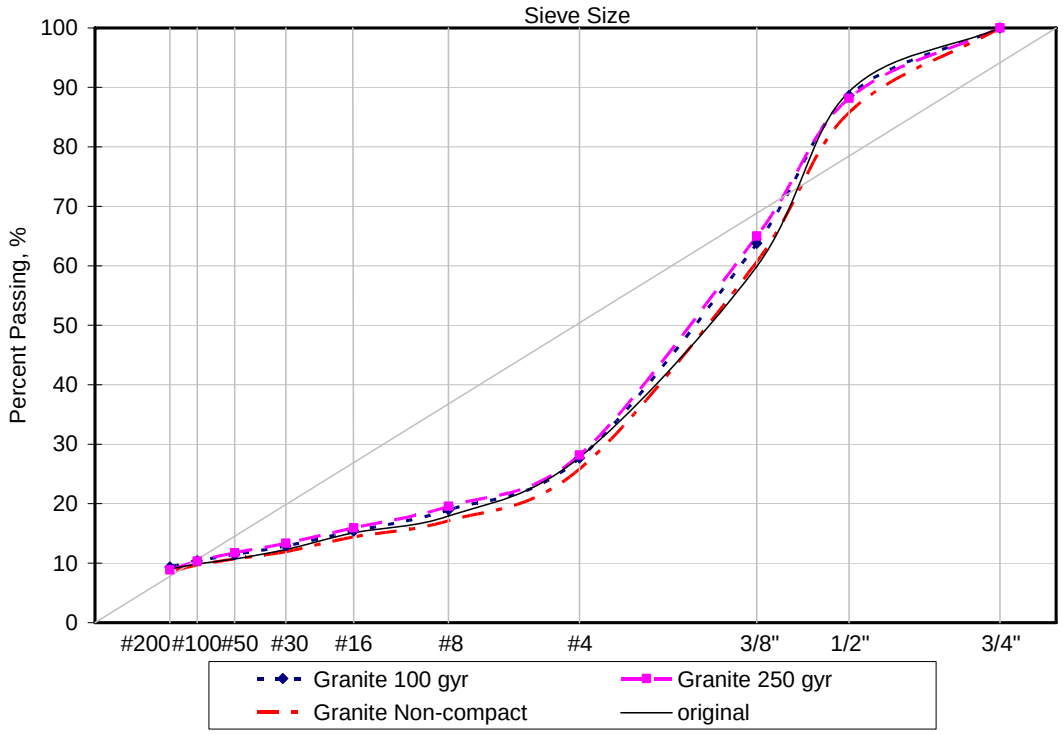

Figure 4.6: Sieve Analysis Results for Granite.

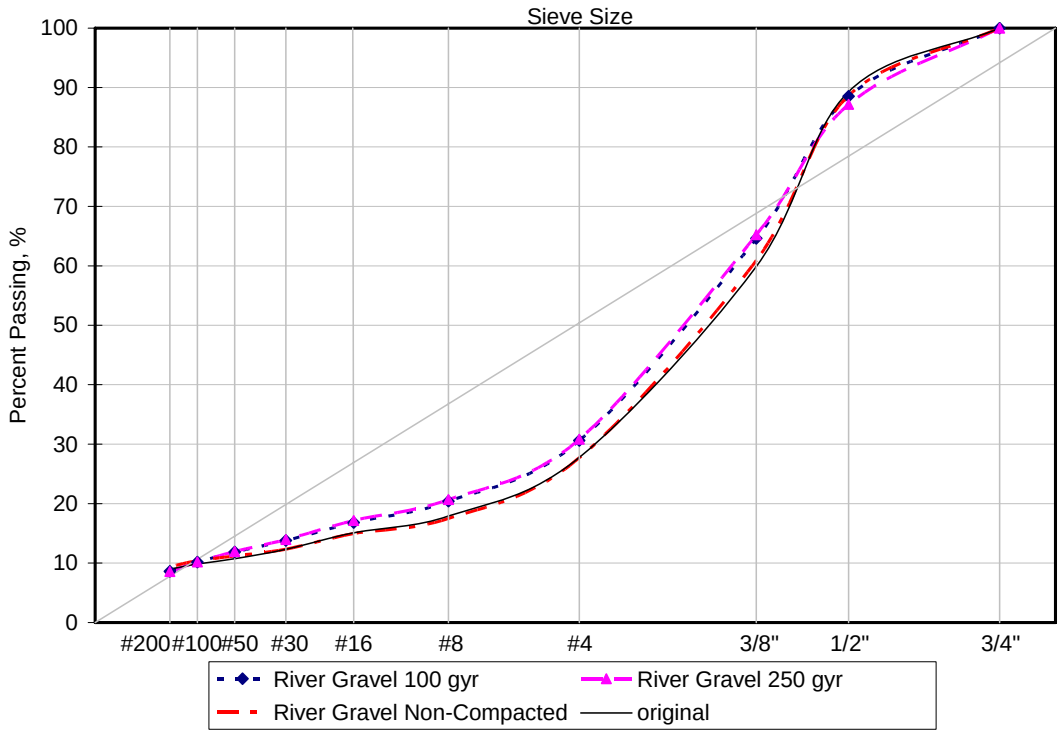

Figure 4.7: Sieve Analysis Results for Uncrushed River Gravel.

In order to better summarize aggregate degradation due to compaction, emphasis of the analysis pertained to the amount retained on the 9.5 mm (3/8 inch) and the 4.75 mm (#4) sieves. The results of the gradation analyses for all mixtures are shown on Figure 4.8. Ideally, a mix design gradation should not change from its design requirement after compaction. However, changes in gradations do occur to different extents after compaction. Once stone-on-stone contact is existent during compaction, the coarse aggregate is exposed to higher shear stresses due to the aggregate interaction. As a result, the coarse aggregate breaks down into intermediate-sized particles, which are further broken down into finer aggregate due to the shear stresses from compaction.

The graph shows the resultant change, with respect to the loose mix gradations, of the aggregates passing the 12.5 mm (1/2 inch) sieve and retained on the 9.5 mm (3/8 inch) sieve and aggregates passing 9.5 mm but retained on the 4.75 mm (#4) sieve for the six mixtures. The 9.5 mm and 4.75 sieve sizes experienced the most change when compared to the other sieve sizes. In fact, these two sizes comprise the majority of the coarse aggregates in addition to being a contributing factor in developing the coarse aggregate structure. Limestone 1 mixture had the most change, while the granite mixture had the least. Limestone 2 followed limestone 1 in terms of change in gradation; however limestone 1 had an increase of 5 percent in the amount retained on the 4.75 mm sieve as opposed to limestone 2, which showed very little change on the same sieve size. Each mixture showed a negative change in 12.5 – 9.5 mm aggregates and a small increase in the 9.5 – 4.75 mm aggregates at 250 gyrations.

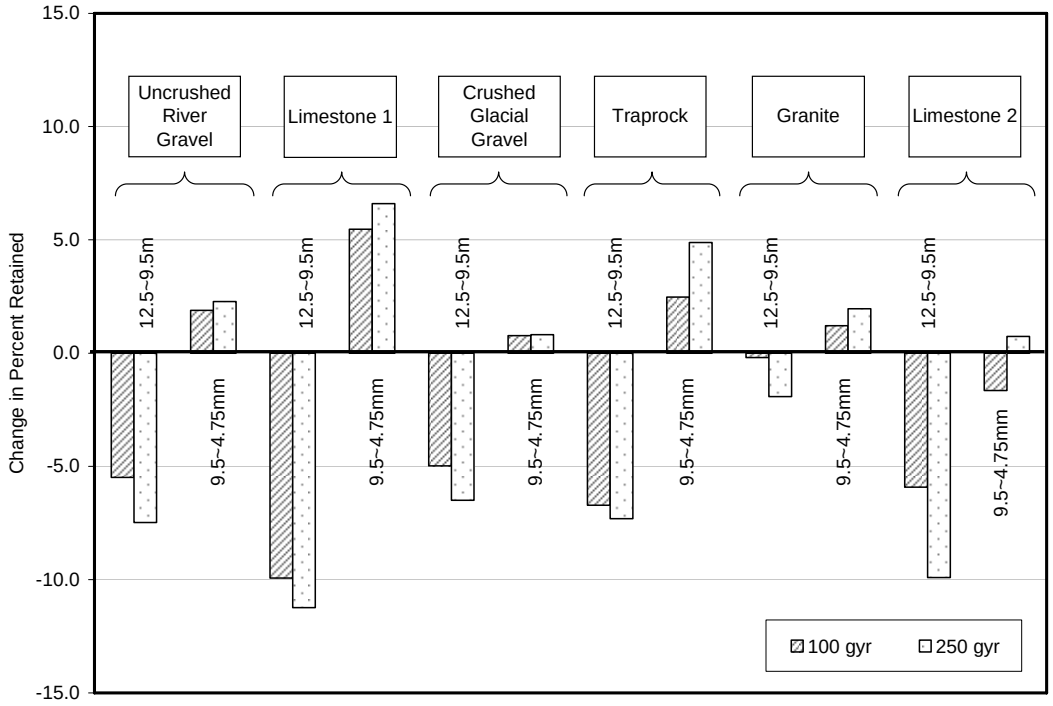

Figure 4.8: Percent Change in 9.5 mm and 4.75 mm Sieves Using Sieve Analysis.

Mixture Stability during Compaction Using Contact Energy Index (CEI)

CEI results for each of the samples and aggregate type are listed in Table 4.2. Further details about the CEI results can be referenced in Appendix A3. The aggregates yielding the highest and lowest CEI values are the glacial gravel at 21 and traprock at 17, respectively. A recent study by Bahia et al. recommends a minimum CEI value of 15 for a mixture designed for high traffic demands (*23*). Based on this recommendation, all six mixtures exceeded the minimum value. Although all the mixtures report CEI values greater than 15, the N_{G1} values varied among the mixtures. N_{G1} is the number of gyrations at which the change in slope of two consecutive gyrations for the percent air

voids versus number of gyrations is less than or equal to 0.001 percent. The river gravel reports the lowest N_{G1} value of 18, while limestone 2 reports the highest at 36.

Table 4.2: CEI Results of Five Aggregates.

Aggregate Type:	Average Values		
	CEI	N_{G1} =	N_{G2} =
Glacial Gravel	21.1	33	233
Granite	20.7	23	223
Limestone 1	20.1	32	232
River Gravel	19.7	18	218
Traprock	17.4	26	226
Limestone 2	19.8	36	236

The shear stress recorded by the SGC is graphed with respect to the number of gyrations in Figure 4.9. A table of a sample of the data obtained from the SGC can be referenced in Appendix A3. The shear stress continued to increase until approximately 70 gyrations. From 70 gyrations to 250 gyrations, the traprock, granite, and river gravel mixtures either stabilized or showed a slight decrease in shear stress. The glacial gravel and the two limestone mixtures showed a decrease in the slope, where limestone 2 exhibited the most reduction in shear stress applied. Limestone 1 and the glacial gravel showed that both had similar shear stresses induced on the specimens, yet limestone 1 had a larger decrease of slope for shear stress applied.

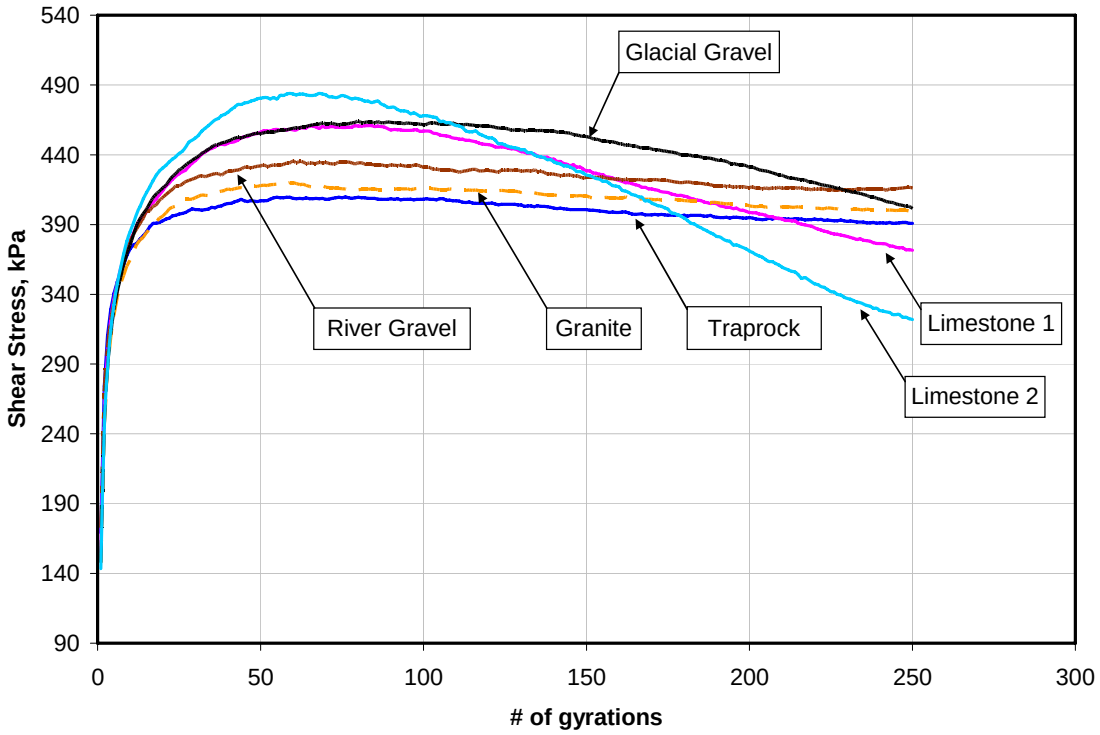

Figure 4.9: Recorded Shear Stress for Mixtures from the SGC.

Aggregate Size Analysis Using Imaging Techniques

The median (50th percentile) of the weight retained on each coarse aggregate sieve size among all images was calculated, and the difference in the median between specimens compacted at 100 gyrations and 250 gyrations was then determined. The results are shown in Figure 4.10. The percentage of aggregates retained on the 12.5 mm (1/2 inch) sieve was small and any change in size would exaggerate the percent change between the two sets of specimens. Therefore, this sieve was not included in the analysis. Negative changes mean the 250 gyration specimens yielded lower counts of aggregate for each respective sieve size. This is typically due to aggregates breaking down and being retained on a smaller sieve. A positive change shows that the specimens

exhibited a higher percentage in that particular size, which is due to larger aggregate breaking into sizes that fall into the respective sieve size. During the analysis of the images, a minimum of 100 images were analyzed for each specimen. It was important to observe the overall distribution of the aggregate sizes in the analysis. The 25^{th} and 75^{th} percentiles of the data were plotted to show if the results of the analysis were skewed. These figures can be referenced in Appendix A4.

Looking at the plots in Figure 10, five out of six aggregates show negative changes. This is particularly the case for the aggregates retained on the 4.75 mm (#4) and 9.5 mm (3/8 inch) sizes. When focusing on the changes in the 9.5 mm, the results indicate that limestone 2 experienced the most change, followed by limestone 1, crushed glacial gravel, uncrushed river gravel, and then granite. The traprock actually showed an increase in aggregate size. This increase is attributed to the error in separating aggregate particles, as it was more difficult to separate particles at the 250 gyration level, due to the increase in contacts, than at the 100 gyration level. Particles that are in contact are considered as one large particle by image analysis techniques. The threshold values for the images obtained for the specimens compacted to 250 gyrations were increased by a value of five, which is approximately a 2 percent increase of filtration. This increase was needed to further separate the particles in contact because the aggregates in the 250 gyration specimens were more packed together as opposed to the 100 gyration specimens. As discussed earlier, particle separation was performed to minimize this error.

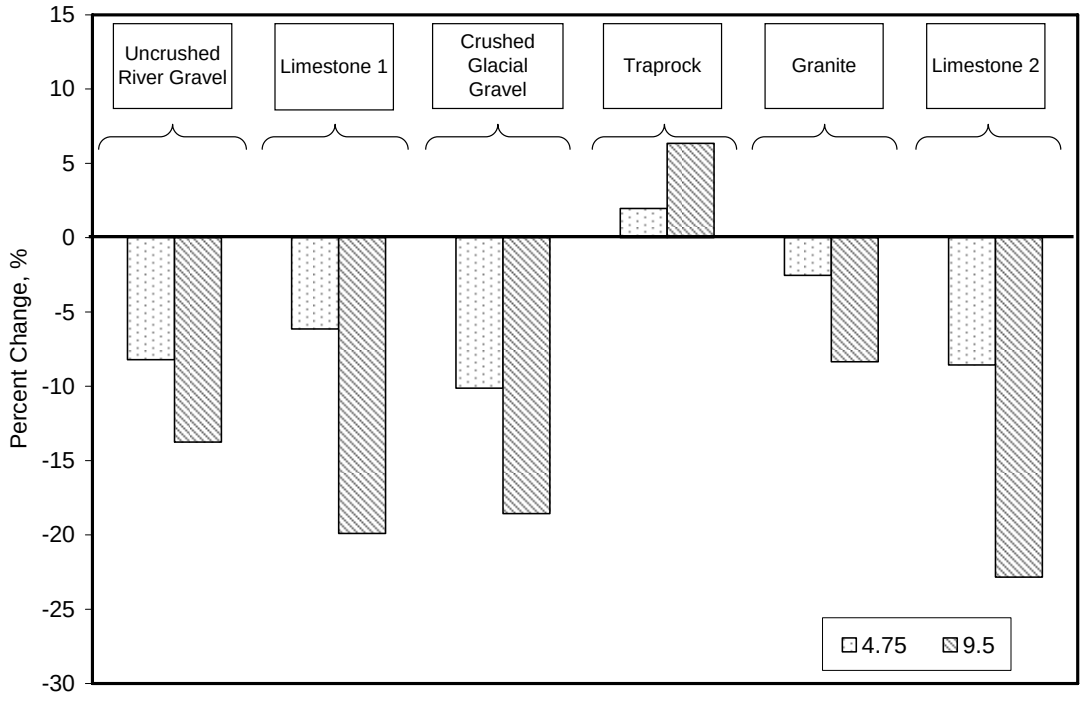

Figure 4.10: Results of Change in Gradation Using X-Ray CT Imaging.

The uncrushed river gravel, crushed glacial gravel and limestone 2 showed similar trends as the respective aggregate size decreased. All three exhibited a large amount of breakdown in the 9.5 mm (3/8 inch) sized aggregate and have moderate breakdown on the 4.75 mm (#4) sized aggregate. As a specimen is compacted, the aggregate come into contact with each other, causing friction, and eventually the aggregate begins to chip or break down. As a result of the aggregate breaking down, particle sizes become smaller.

The granite displayed a different distribution of change in aggregate size. Breakdown was apparent for the 9.5 mm (3/8 inch) retained, but there was little change for the 4.75 mm (#4) aggregate. Because granite is a strong and elongated aggregate, the

resultant sizes due to the breakdown of the 9.5 mm (3/8 inch) sized aggregate consists primarily of 4.75 mm (#4) sized particles causing the results to show minor changes. Furthermore, the 9.5 mm (3/8 inch) is not necessarily crushing but being chipped. These chipped particles would primarily consist of 4.75 mm (#4) sized aggregate and because of their strength show little crushing as opposed to the other aggregate types.

Aggregate Degradation Due to Repeated Dynamic Loading

The aggregate gradations after flow number testing were compared to the gradations of control samples that were not tested with the flow number test. Changes in aggregate gradations due to dynamic loading are shown in Figure 4.11. The results revealed no significant change in gradations before and after the flow number test. Four of the specimens showed minor aggregate breaking in the 9.5 mm (3/8 inch) sieve while showing an increase on the 4.75 mm (#4) retained. Granite exhibited the most degradation in the test, while the limestone 2 had the least. It was also found that the mixtures with higher asphalt content yielded lower flow number values. The gradations obtained from the laboratory results can be referenced in Appendix A5.

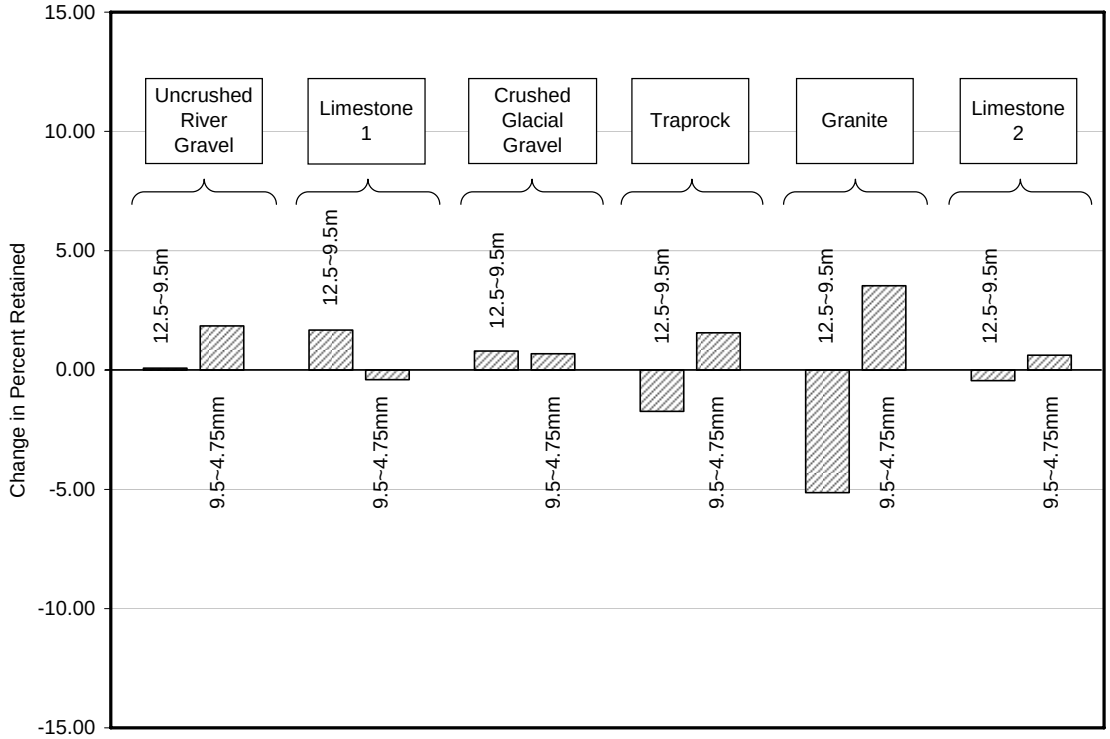

Figure 4.11: Percent Change in 9.5 mm and 4.75 mm Sieves for the Flow Number Test.

Analysis of Results and Discussion

The aggregate interaction within SMA is crucial to ensuring that the asphalt mix will perform well under field conditions. One of the factors that affects the performance of SMA is the quality of aggregate. Much of the performance of SMA is dependent on the quality of aggregate and its resistance to degradation. The results presented in this chapter provide interesting data that relate aggregate characteristics to degradation in SMA.

Aggregate breakdown was evident in all mixtures to different levels. Aggregates of the 12.5 mm (1/2 inch) to 9.5 mm (3/8 inch) fraction decreased as shown on Figure

4.8. All mixtures that exhibited breakdown in the 9.5 mm (3/8 inch) sieve showed that they were retained on the 4.75 mm (#4) sieve, which explains the increase in some retained material. Out of the six mixtures, limestone 1 exhibited the greatest amount of aggregate breakdown in the 9.5 mm sieve, followed by limestone 2, glacial gravel, and then river gravel (Figure 4.8). The granite mixture showed a change in gradation, but it was small compared to the other five mixtures. Figure 4.8 also shows that the gradations of the aggregates were affected by the increased number of gyrations from 100 to 250. Limestone 2 mixture was most affected by the increased gyrations.

The Micro-Deval test result showed that the two limestone samples exhibited the most percent loss (Table 4.1). Looking at the results of the Micro-Deval test on Table 4.1, it shows that the limestone 1 and 2 results support the outcome of the gradation in Figures 4.4 and 4.5, implying that degradation has occurred. It is evident that the limestone mixtures are experiencing breakdown due to increased compaction. This is also true for the glacial gravel, as it had similar Micro-Deval values to the limestone mixtures. On the other hand, the sieve analysis results for the granite mixture correlated well with the Micro-Deval results. This mixture showed the least change in gradation due to compaction (Figures 4.6 and 4.8) as well as exhibiting a low percent loss due to the Micro-Deval test.

The CEI values for all mixtures exceeded the minimum CEI value of 15 (*23*). Therefore, CEI could not be used to detect aggregate degradation. Shear stress measurements showed that the two limestone mixtures and the glacial gravel mixture experienced a softening behavior as depicted in the reduction of shear stress with an

increase in number of gyrations. These results support the findings from the change in gradation using the imaging techniques and, to some extent, the results of the mechanical sieve analysis.

Looking at the results of the Micro-Deval test on Table 4.3, the two limestone samples exhibit the highest percent loss, followed by the traprock, glacial gravel, granite , and river gravel. The Micro-Deval results (Table 4.1) of limestone 2 support the results of the change in gradation in Figure **4.**8, showing that breakdown has occurred. It is evident that the limestone mixtures experienced breakdown due to compaction. Also, the granite was a mix where the results of the post-compaction gradation correlated well with the Micro-Deval results. This mix showed the least change in gradation due to compaction (Figure 4.8) as well as the least percent weight loss in the Micro-Deval.

Limestone 2 is softer than limestone 1, which is supported by the Micro-Deval results. However, Figure 4.8 shows that breakdown of limestone 2 was less than that of limestone 1 when compacted to 100 gyrations. Limestone 2 had nearly the same amount of change in the 9.5 mm (3/8 inch) sieve as limestone 1 when compacted to 250 gyrations. The imaging results in Figure 4.10 support the mechanical sieve analysis finding, as the difference between the two limestone mixes was very small. It is evident that the difference between these two aggregates in the Micro-Deval did not translate into gradation analysis. Micro-Deval results are determined by the weight loss through the 1.18 mm (#16) sieve. Breakdown may alter the distribution of aggregates used in the Micro-Deval test, but the breakdown may be limited to sizes larger than 1.18 mm. This

would be the case for the limestone 1. In comparison to limestone 2, abrasion caused a large percentage of aggregates to pass sieve 1.18 mm (#16) sieve.

The AIMS results can be used to help explain the findings from the Micro-Deval test and gradation analysis. Limestone 1 experienced a small change in angularity (Figure 4.1a), while the change in sphericity was significant. Past experience with AIMS results has shown that a change in sphericity is an indication of particles' breakage, while a change in angularity indicates loss of angular elements on the surface, which tend to be smaller than those produced due to breakage. The change in texture is not indicative of weight loss, as texture is measured at very high resolution (*27*), and its changes correspond to the loss of a very small amount of fine particles that are typically pass the 0.075 mm (#200) sieve. These AIMS results indicate that limestone 1 experienced breakage to relatively large pieces rather than abrasion that would produce particles passing 1.18 mm (#16) sieve. However, limestone 2 became less elongated after Micro-Deval due to the abrasion of its surface.

The remaining aggregates (uncrushed river gravel, crushed glacial gravel, and granite) experienced some aggregate breakdown as indicated in Figures 4.2, 4.6 and 4.7. However, the small changes in Micro-Deval loss (less than 12 percent) along with the small changes in sphericity (Figure 4.1b) indicate that these changes are not significant. However, it is interesting to note the trends exhibited by the traprock. Figure 4.3 shows that the traprock mixture was not subject to major crushing at either 100 or 250 gyrations; however, the traprock had a moderate loss of 11.3% due to the Micro-Deval test. Furthermore, Figure 4.9 shows that limestone 2 experienced a larger amount of

shear stress compared to the other mixes when compacted to 250 gyrations, yet Figure 4.9 shows that the gyratory compactor recorded a lower shear stress.

When the results from compaction analysis were compared to the results of the flow number test, no correlation could be established. There was no significant change in gradation as a result of the specimens subjected to dynamic loading. One possible explanation could be that the applied stress (310 kPa) was not high enough to cause aggregate breakdown. Moreover, the tests were conducted in an unconfined condition for simplicity. In unconfined condition, the permanent deformation of the SMA specimen was probably mostly due to the plastic flow of mastic.

Approach for the Analysis of Aggregate Breakage and Abrasion

This section presents an approach for the analysis of aggregate breakage and abrasion. The limits that are included herein need to be further examined in future studies based on the relationship of aggregate abrasion and fracture or breakage to SMA performance. Nonetheless, this approach is presented here to set the framework for the development of this linkage.

Figure 4.12 shows the relationship between percent change in weight retained on the aggregate size smaller than the NMAS versus weight loss in the Micro-Deval. Only a small weight is retained on the NMAS, and, consequently, evaluating weights on the NMAS would exaggerate the percent change due to compaction. Aggregates in region A exhibit small changes in gradation and small Micro-Deval loss; these aggregates are expected to resist degradation in SMA. Aggregates in region B experience change in

gradation due to compaction, but they have small loss in Micro-Deval. These types of aggregates could be susceptible to fracture under compaction, but they resist surface abrasion and loss of angularity. It is recommended that mix design engineers conduct an evaluation of aggregate gradation even on those that meet the Micro-Deval requirements to ensure aggregate resistance to degradation. Aggregates in region C have high Micro-Deval loss, and they are susceptible to degradation in SMA. Aggregates that would fall in region D are those that have high Micro-Deval loss, but HMA can be designed such that aggregate degradation is minimized (low change in gradation). Even if aggregates do not meet the allowable weight loss requirements in the Micro-Deval, they can still be used if the change in gradation is minimized to acceptable limits.

Neither the Micro-Deval test nor the aggregate gradation analysis can capture the changes in texture, which is an important aspect of aggregate degradation in SMA. Therefore, the AIMS can also be used to evaluate this aspect of aggregate degradation. For example, the limestone 1 aggregate experienced the highest loss of texture as evident in Figure 4.1c. Current research is focusing on establishing the limits in this approach based on evaluation of aggregate gradation in cores from asphalt pavements and SMA laboratory and field performance.

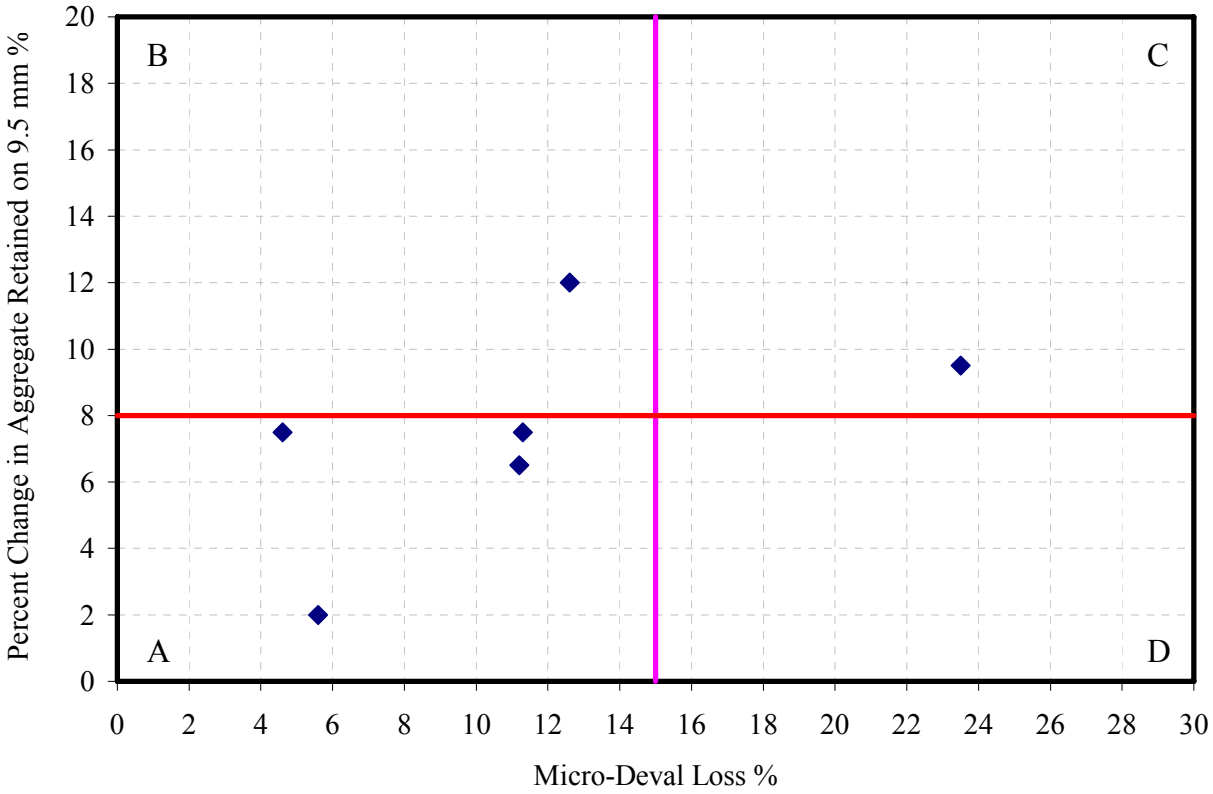

Figure 4.12: The Relationship between Change in Aggregate Gradation and Micro-Deval Loss.

CHAPTER V
CONCLUSIONS AND RECOMMENDATIONS

It is recommended to use the weight loss in the Micro-Deval, the change in aggregate shape characteristics, and the change in gradation to evaluate the resistance of aggregate particles to degradation in SMA mixes.

The measurement of weight loss in the Micro-Deval combined with the change in gradation due to compaction can be very valuable procedures to evaluate the resistance of aggregates to degradation. Even if aggregates do not meet the allowable weight loss requirements in the Micro-Deval, they can still be used if the change in gradation is minimized to acceptable limits. On the other hand, aggregates that exhibit small weight loss should be evaluated for possible degradation in the mix and should be avoided if proven to be susceptible to breakage.

AIMS can be used to supplement the Micro-Deval results. A decrease in sphericity indicates that the aggregate has the potential to experience particle breakage. AIMS results can also be used to set maximum values for loss of texture in order for the mix to have the necessary friction between particles.

X-ray CT is a research tool that was used in this study to confirm the findings from the mechanical analysis of aggregate gradation after compaction. In general, the findings from X-ray CT were consistent with those from mechanical sieve analysis.

The flow number test is a destructive test that measures the number of dynamic loads applied to an asphalt mixture that causes tertiary permanent deformation. However, it may not be an efficient means to test for aggregate degradation. Future

research is needed to determine if the flow number test is capable of testing SMA specimens in both an unconfined and confined condition. Also, further study is needed to see if the high asphalt content of SMA specimens has an effect on the flow number.

Future Research

While performing the laboratory testing and data analysis, several issues arose that would suggest a need for further research or improvement. These issues are listed below:

- As previously mentioned in Chapter IV, an approach is introduced that helps analyze aggregate breakage and abrasion. It is suggested to establish a relationship between the amount of breakdown in the sieve analysis versus the abrasion loss obtained from the Micro-Deval. The relationship can be used to determine parameters for the selection of aggregates that are suitable for a high-quality asphalt mixture (i.e., SMA) by means of their shape properties and performance.
- It is recommended that future studies for aggregate degradation in SMA focus on establishing a database of current aggregates used in SMA. This database would include the laboratory and field results of these SMA pavements, as well as the shape characteristics and their performance results (i.e., Micro-Deval, AIMS) of the coarse aggregates used in the mixtures.
- The flow number test has proven to be a useful test to determine pavement performance. However, it was found that additional research is needed to

establish whether this test is suitable for SMA in both a confined and unconfined condition. It would also be beneficial to analyze the effect of high asphalt contents and its relationship to flow number.

- The L.A. abrasion test is the current test specified in the AASHTO design of SMA mixtures. It would be recommended to consider the Micro-Deval abrasion test as a suitable alternative for testing of aggregate degradation. Furthermore, it is recommended that the findings in this study would be used to establish a design approach for SMA that would have an increased focus on aggregate degradation.

REFERENCES

1. Brown, E.R. *Experience with Stone Matrix Asphalt in the United States*. NCAT Report No. 93-4. National Center for Asphalt Technology, Auburn University, Auburn, Ala., 1992.

2. Bellin, P. Development, Principles and Long-Term Performance of Stone Mastic Asphalt in Germany. In *SCI Lecture Papers*, No. 87, SCI Journals, London, United Kingdom, 1997.

3. Lynn, T.A. *Evaluations of Aggregate Size Characteristics in Stone Matrix Asphalt (SMA) and Superpave Design Mixtures*. Ph.D Dissertation. Auburn University, 2002.

4. *AASHTO Provisional Standards*. American Association of State Highway and Transportation Officials, Washington D.C., 2001.

5. Xie, H., and D.E. Watson. Determining Air Voids Content of Compacted Stone Matrix Asphalt Mixtures. In *Transportation Research Record: Journal of the Transportation Research Board*, No. 1891 TRB, National Research Council, Washington D.C., 2004, pp.203-211.

6. Xie, H., and D.E. Watson. *Lab Study on Degradation of Stone Matrix Asphalt (SMA) Mixtures*. Presented at the 83rd Annual Meeting of the Transportation Research Board, Washington D.C., 2004.

7. Brown, E.R., J.E. Haddock, R.B. Mallick, and T.A. Lynn. *Development of a Mixture Design Procedure for Stone Matrix Asphalt (SMA)*. NCAT Report No. 97-3. National Center for Asphalt Technology, Auburn University, Auburn, Ala., 1997.

8. Brown, E.R. and J.E. Haddock. *A Method to Ensure Stone-on-Stone Contact In Stone Matrix Asphalt Paving Mixtures*, NCAT Report No. 97-2. National Center for Asphalt Technology, Auburn University, Auburn, Ala., 1997.

9. Watson, D.E., E. Masad, K.A. Moore, K. Williams, and L.A. Cooley. Verification of VCA Testing to Determine Stone-On-Stone Contact of HMA Mixtures. In *Transportation Research Record: Journal of the Transportation Research Board*, No. 1891 TRB, National Research Council, Washington D.C., 2004, pp. 182–190.

10. Brown, E.R., and R.B. Mallick. *Stone Matrix Asphalt-Properties Related to Mixture Design*. NCAT Report No. 94-2. National Center for Asphalt Technology, Auburn University, Auburn, Ala., 1994.

11. Brown, E.R., and R.B. Mallick. Laboratory Study on Draindown of Asphalt Cement in Stone Matrix Asphalt. In *Transportation Research Record: Journal of the*

Transportation Research Board, No. 1513, TRB, National Research Council, Washington D.C., 1995, pp.25-38.

12. Masad, E. X-Ray Computed Tomography of Aggregates and Asphalt Mixes. In *Materials Evaluations Journal*, vol. 62, No. 7, 2004, pp. 775 – 783.

13. Micheal, L., G. Burke, and C.W. Schwartz. Performance of Stone Matrix Asphalt Pavements in Maryland. In *Journal of the Association of Asphalt Paving Technologists*, Vol. 72, 2003, pp. 287-314.

14. Prowell, B.D., L.A. Cooley Jr, and R.J. Schreck. Virginia's Experience with 9.5-mm Nominal-Maximum-Aggregate-Size Stone Matrix Asphalt. In *Transportation Research Record: Journal of the Transportation Research Board*, No. 1813, TRB, National Research Council, Washington D.C., 2002, pp. 133-141.

15. Watson, D.E. Updated Review of Stone Matrix Asphalt and Superpave Projects. In *Transportation Research Record: Journal of the Transportation Research Board*, No. 1832, TRB, National Research Council, Washington D.C., 2003, pp. 217-223.

16. *NAPA Design and Constructing SMA Mixtures – State-of-the-Practice*. National Asphalt Pavement Association, Lanham, Maryland, 2002.

17. Schmiedlin, R.B., and D.L. Bischoff. *Stone Matrix Asphalt the Wisconsin Experience*. WisDOT Report No. WI/SPR-02-02. Wisconsin Department of Transportation, Division of Transportation Infrastructure Development, Bureau of Highway Construction, Technology Advancement Unit, Madison, Wisconsin, 2001.

18. Brown, E.R., and R.B. Mallick. Evaluation of Stone-on-Stone Contact in Stone Matrix Asphalt. In *Transportation Research Record: Journal of the Transportation Research Board*, No. 1492, TRB, National Research Council, Washington D.C., 1995, pp. 208-219.

19. Moavenzadoh, F., and W.H. Goetz. Aggregate Degradation in Bituminous Mixtures. In *Highway Research Record*, HRB, No. 24, National Research Council, Washington D.C., 1963, pp. 106-137.

20. Aho, B.D., W.R. Vavrick, and S.H. Carpenter. Effect of Flat and Elongated Coarse Aggregate on Field Compaction of Hot-Mix Asphalt. In *Transportation Research Record: Journal of the Transportation Research Board*, No. 1761 TRB, National Research Council, Washington D.C., 2001, pp. 26-31.

21. Dessouky, S., E. Masad, and F. Bayomy. Evaluation of Asphalt Mix Stability Using Compaction Properties and Aggregate Structure Analysis. In *International Journal of Pavement Engineering*, Vol. 4, No. 2, 2003, pp. 87 -103.

22. Dessouky, S., E. Masad, and F. Bayomy. Prediction of Hot Mix Asphalt Stability Using the Superpave Gyratory Compactor. In *Journal of Materials in Civil Engineering*, ASCE, Vol. 16, No. 6, 2004, pp. 578 – 587.

23. Bahia, H., E. Masad, A. Stakston, S. Dessouky, and F. Bayomy. Simplistic Mixture Desin Using the SGC and the DSR. In *Journal of the Association of Asphalt Paving Technologists*, Vol. 72, 2003, pp.196-225.

24. Senior, S.A., and C.A. Rogers. Laboratory Tests for Predicting Coarse Aggregate Performance in Ontario. In *Transportation Research Record: Journal of the Transportation Research Board*, No. 1301, TRB, National Research Council, Washington D.C., 1991, pp. 97-106.

25. Cooley, L.A., and R.S. James. Micro-Deval Testing of Aggregates in the Southeast. In *Transportation Research Record: Journal of the Transportation Research Board*, No. 1837, TRB, National Research Council, Washington D.C., 2003, pp. 73-79.

26. Fletcher, T., C. Chandan, E. Masad, and K. Sivakumar. Aggregate Imaging System for Characterizing the Shape of Fine and Coarse Aggregates. In *Transportation Research Record: Journal of the Transportation Research Board*, No. 1832, TRB, National Research Council, Washington D.C., 2003, pp. 67-77.

27. Al-Rousan, A., E. Masad, L. Myers, and C. Speigelman. A New Methodology for Shape Classification of Aggregates. In *Transportation Research Record: Journal of the Transportation Research Board*, TRB, National Research Council, Washington D.C., (Accepted for Publication, 2005).

28. Masad, E. The Development of a Computer Controlled Image Analysis System for Measuring Aggregate Shape Properties. *NCHRP-IDEA Project 77 Final Report*, Transportation Research Board, Washington, D.C., 2003.

29. McGahan, J. *The Development of Correlations between HMA Pavement Performance and Aggregate Shape Properties*. Master of Science Thesis. Texas A&M University, College Station, TX, 2005.

30. Brown, E.R. Designing Stone Matrix Asphalt Mixtures for Rut-Resistant Pavements. *NCHRP Project 425 Final Report*, Transportation Research Board, Washington, D.C., 1999.

31. Masad, E., and J.W. Button. Implications of Experimental Measurements and Analyses of the Internal Structure of Hot-Mix Asphalt. In *Transportation Research Record: Journal of the Transportation Research Board*, No. 1891, TRB, National Research Council, Washington D.C., 2004, pp. 212-220.

32. Masad, E., V.K. Jandhyala, N. Dasgupta, N. Somadevan, and N. Shashidhar. Characterization of Air Void Distribution in Asphalt Mixes Using X-Ray CT. In *Journal of Materials in Civil Engineering*. Vol. 14, No. 2, ASCE, Reston, Virginia, 2002.

33. Tashman, L., E. Masad, J. D'Angelo, J. Bukowski, and T. Harman. X-ray Tomography to Characterize Air Void Distribution in Superpave Gyratory Compacted Specimens. In *The International Journal of Pavement Engineering*, Vol. 3, No. 1, 2002, pp. 19-28.

34. Tashman, L., E. Masad, B. Peterson, and H. Saleh. Internal Structure Analysis of Asphalt Mixes to Improve the Simulation of Superpave Gyratory Compaction to Field Conditions. In *Journal of the Association of Asphalt Paving Technologists*, Vol. 70, 2001, pp. 605-645.

35. Witczak, M.W., K. Kaloush, T. Peillinen, M.E. Basyouny, and H.V. Quintus. *Simple Performance Test for Superpave Mix Design*, NCHRP Report No. 465, 2002.

36. Lane, B.C., C.A. Rogers, and S.A. Senior. The *Micro-Deval Test for Aggregates in Asphalt Pavement*. Presented at the 8th Annual Symposium of International Center for Aggregates Research, Denver, CO, 2000.

APPENDIX A1

MICRO-DEVAL AND AIMS RESULTS USED FOR THE ANALYSIS OF AGGREGATE DEGRADATION BY ABRASION

Table A1-1: Micro-Deval Results.

Description	Micr-Deval Loss (%)		
	Sample 1	Sample 2	Average
Limestone 1	12.56	12.51	12.54
Traprock	11.23	11.26	11.25
Crushed Glacial Gravel	11.18	11.13	11.16
Uncrushed River Gravel	4.73	4.54	4.63
Granite	5.51	5.60	5.56
Limestone 2	23.93	23.08	23.50

Table A1-2: AIMS Results Before and After Micro-Deval Test.

Aggregate Type	Angularity-Gradient Method		Sphericity		Texture	
	Before MD	After MD	Before MD	After MD	Before MD	After MD
Uncrushed River Gravel	2227.93	2560.60	0.70	0.68	53.58	58.01
Granite	2768.49	2465.74	0.62	0.58	219.74	263.37
Limestone - 1	2696.82	2423.37	0.65	0.21	203.16	66.03
Crushed Glacial Gravel	2937.94	1999.00	0.60	0.66	160.31	77.07
Traprock	2449.90	1993.22	0.73	0.63	311.81	177.42
Limestone - 2	2157.33	1879.03	0.65	0.70	78.24	47.17

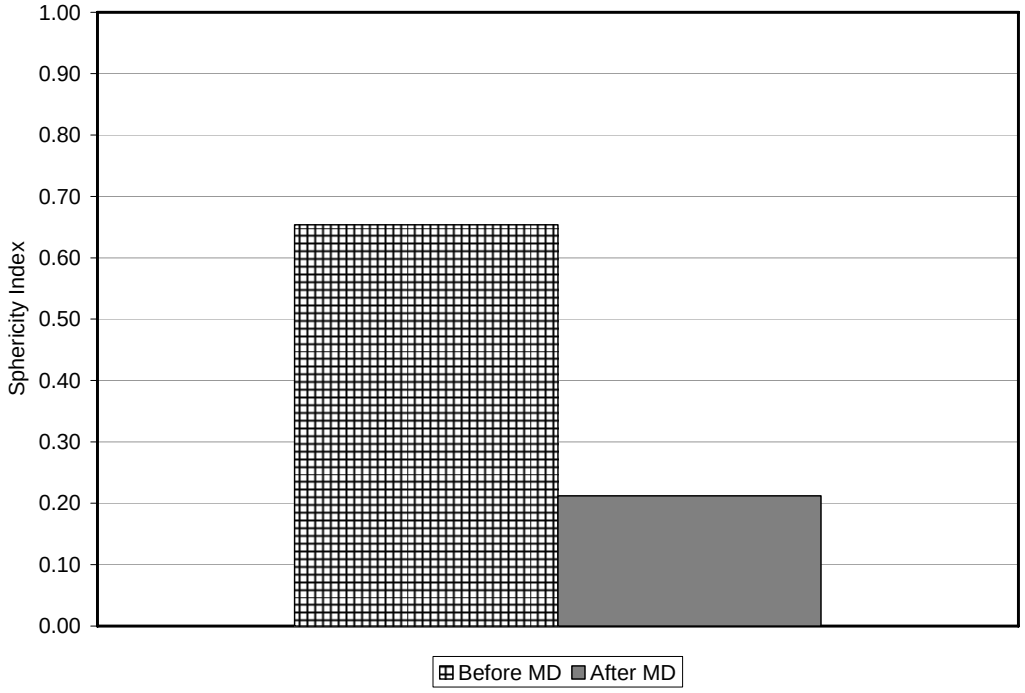

Figure A1-1: AIMS Sphericity Results Before and After Micro-Deval Test for Limestone 1.

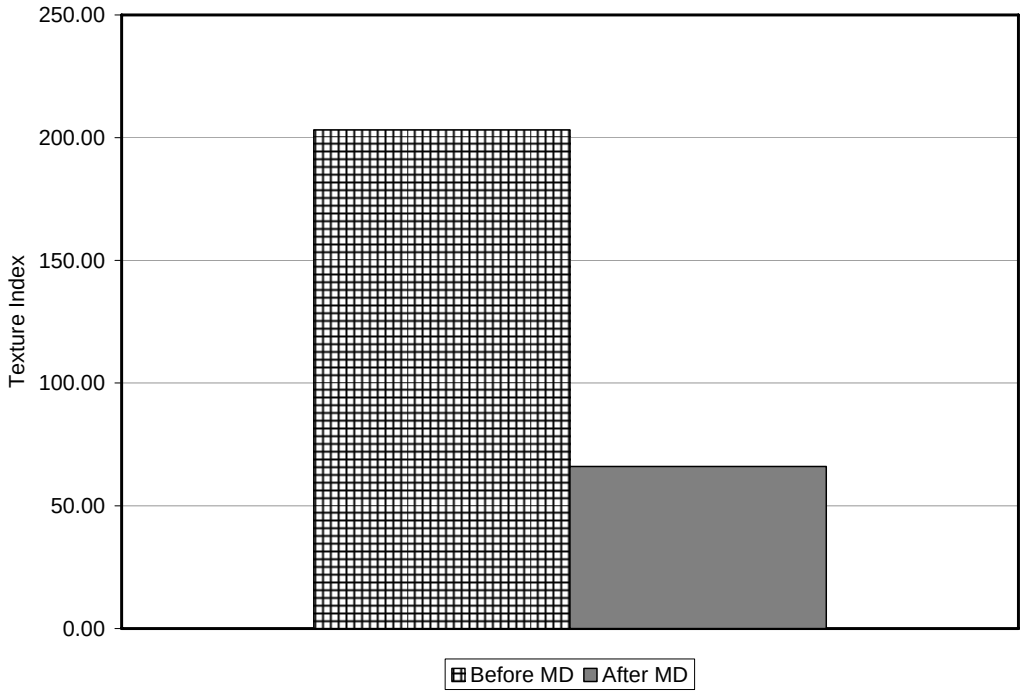

Figure A1-2: AIMS Texture Results Before and After Micro-Deval Test for Limestone 1.

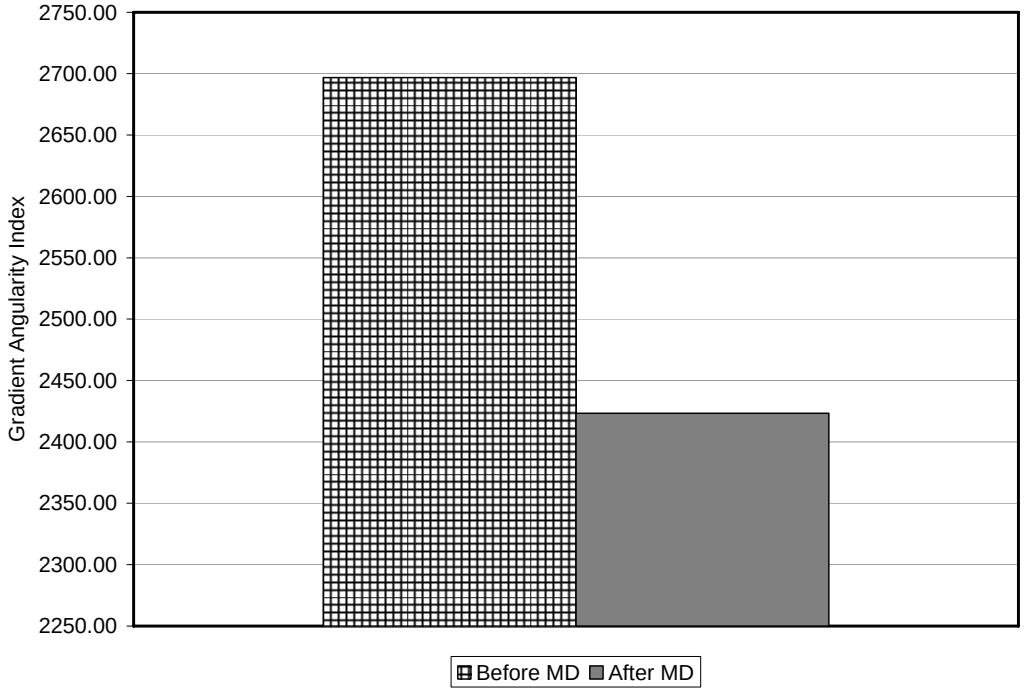

Figure A1-3: AIMS Angularity Results Before and After Micro-Deval Test for Limestone 1.

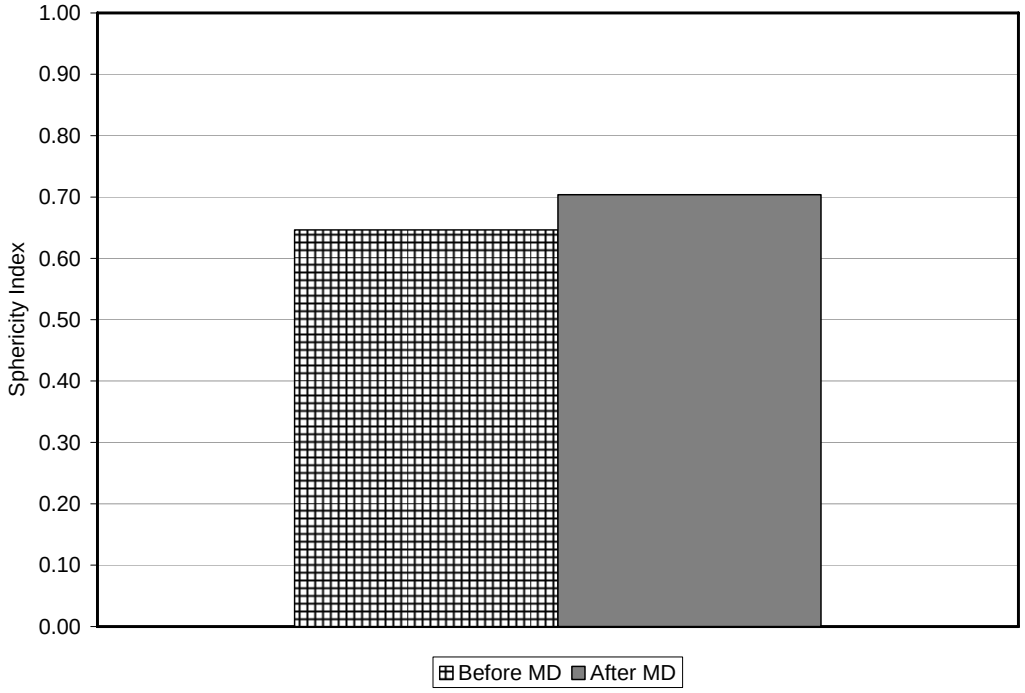

Figure A1-4: AIMS Sphericity Results Before and After Micro-Deval Test for Limestone 2.

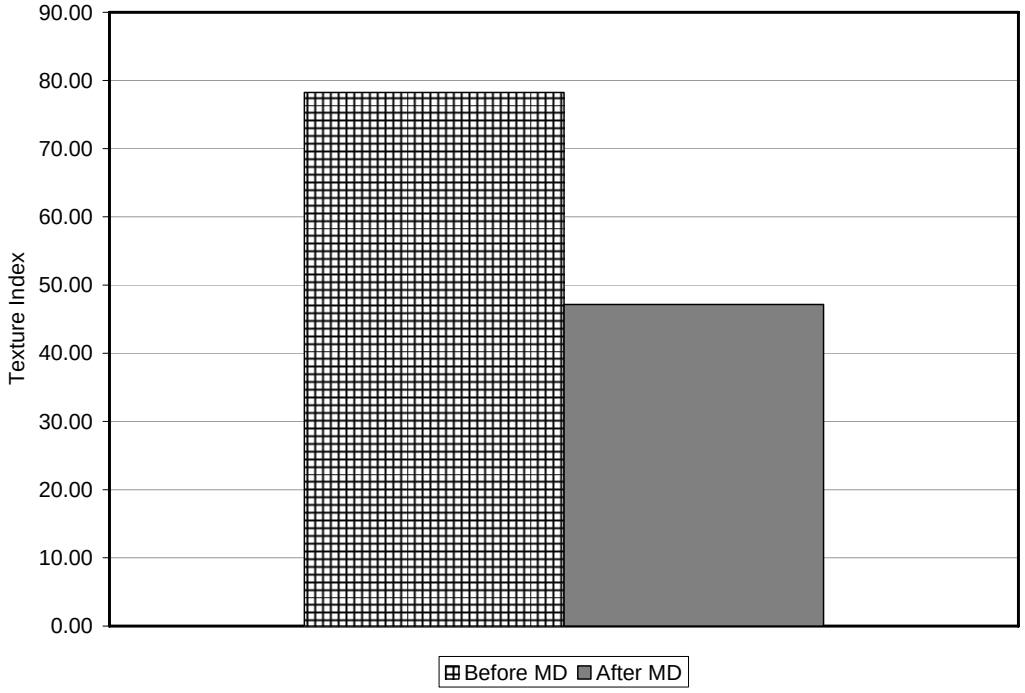

Figure A1-5: AIMS Texture Results Before and After Micro-Deval Test for Limestone 2.

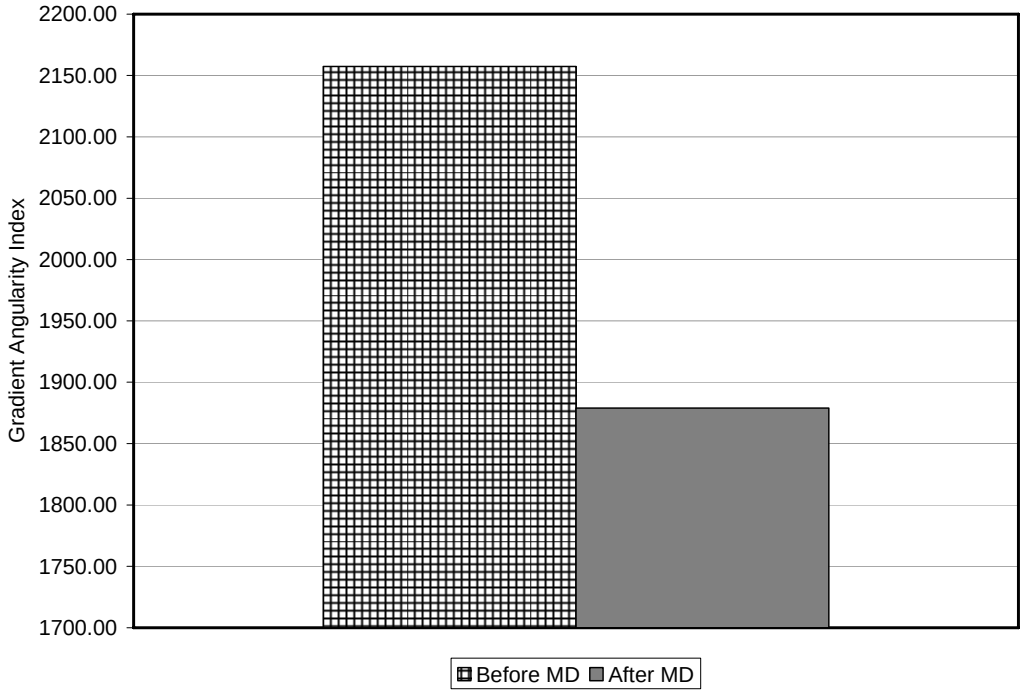

Figure A1-6: AIMS Angularity Results Before and After Micro-Deval Test for Limestone 2.

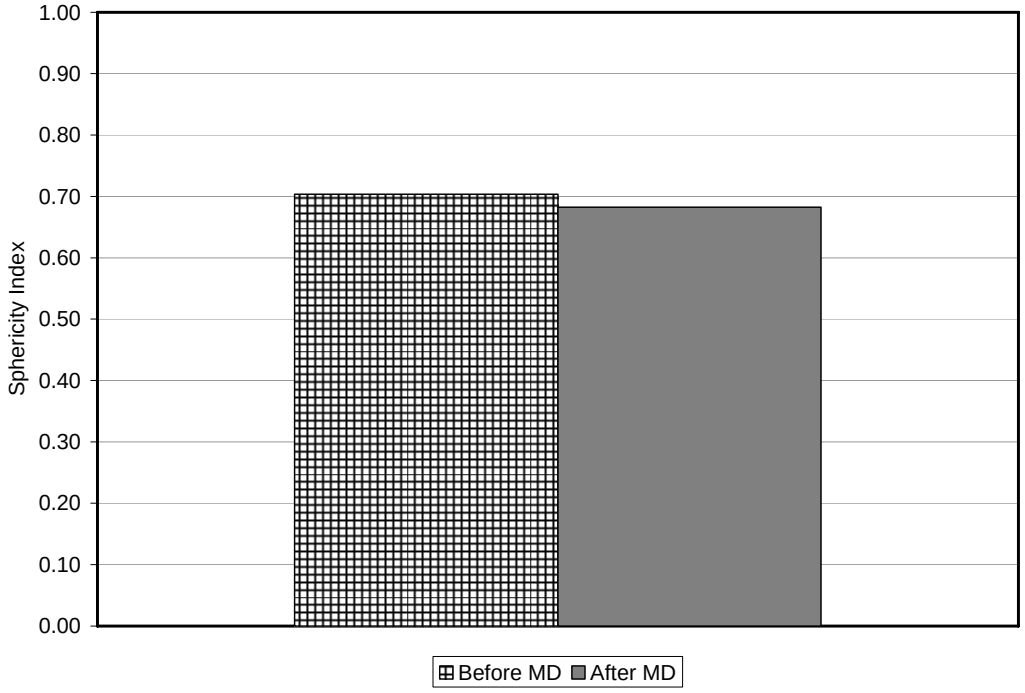

Figure A1-7: AIMS Sphericity Results Before and After Micro-Deval Test for Uncrushed River Gravel.

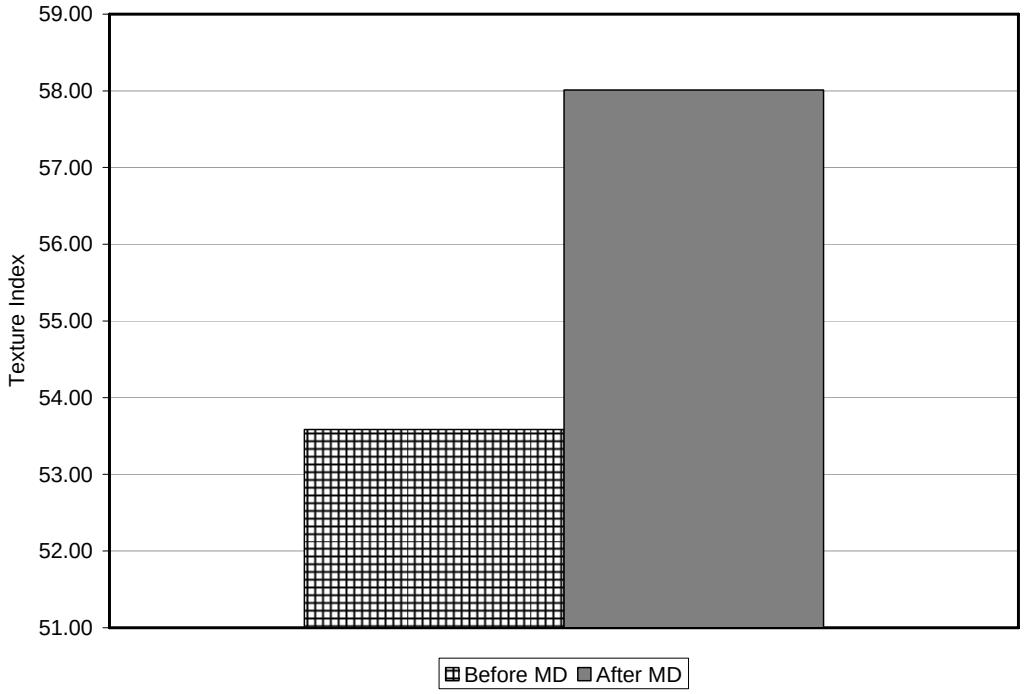

Figure A1-8: AIMS Texture Results Before and After Micro-Deval Test for Uncrushed River Gravel.

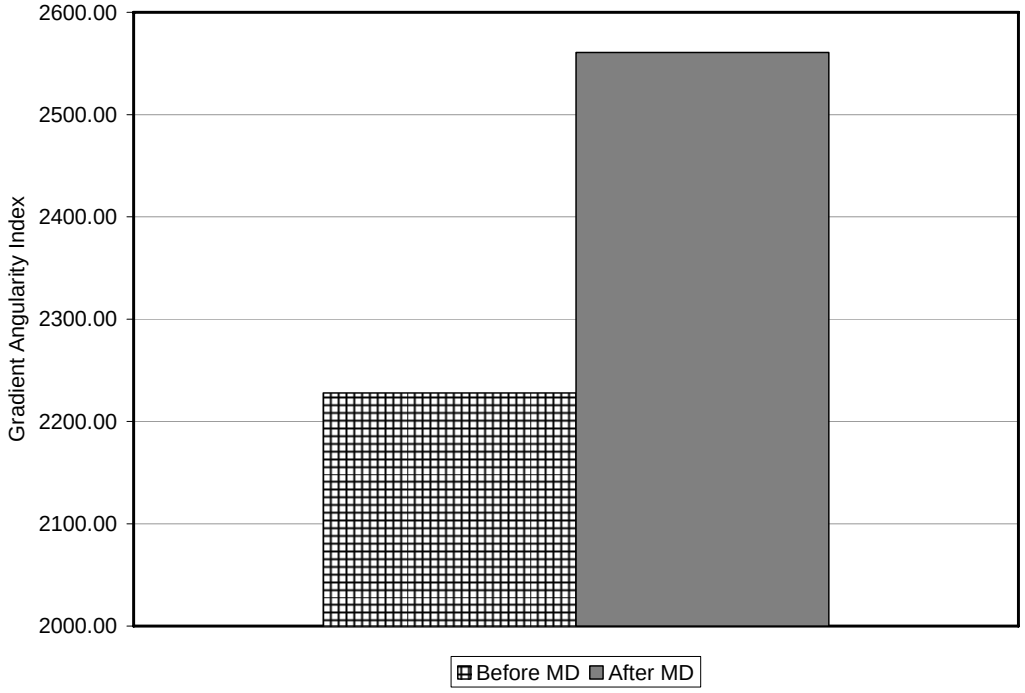

Figure A1-9: AIMS Angularity Results Before and After Micro-Deval Test for Uncrushed River Gravel.

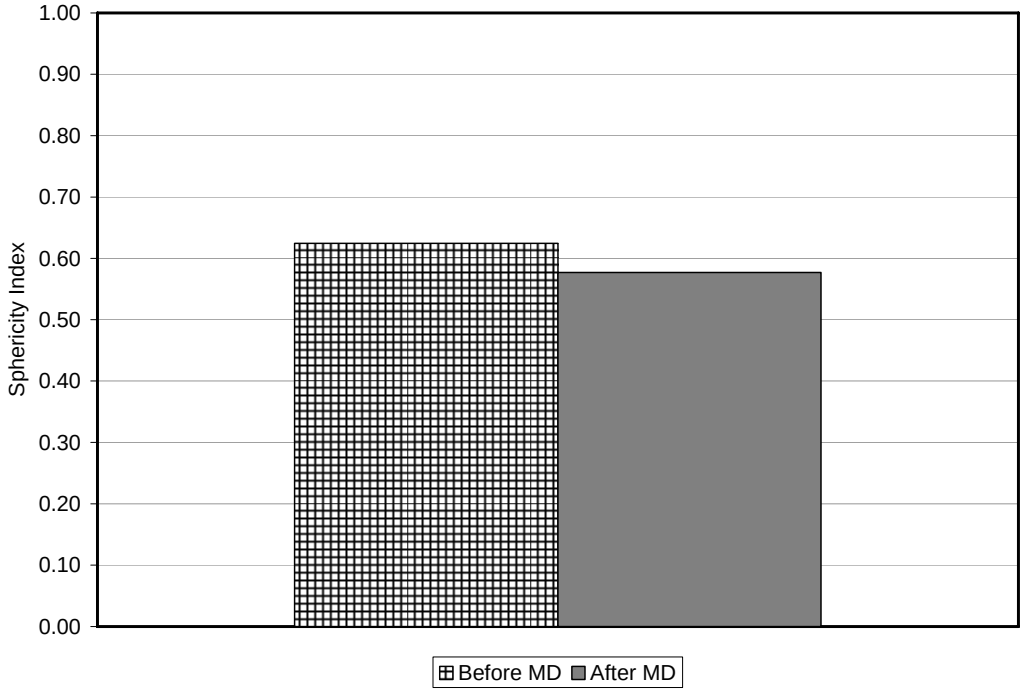

Figure A1-10: AIMS Sphericity Results Before and After Micro-Deval Test for Granite.

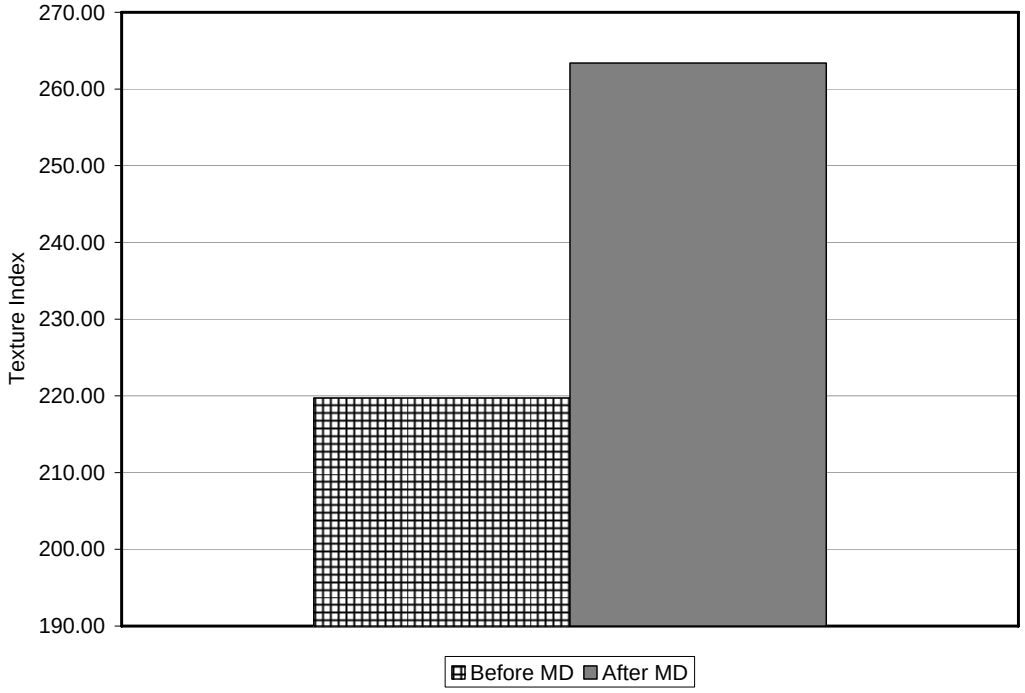

Figure A1-11: AIMS Texture Results Before and After Micro-Deval Test for Granite.

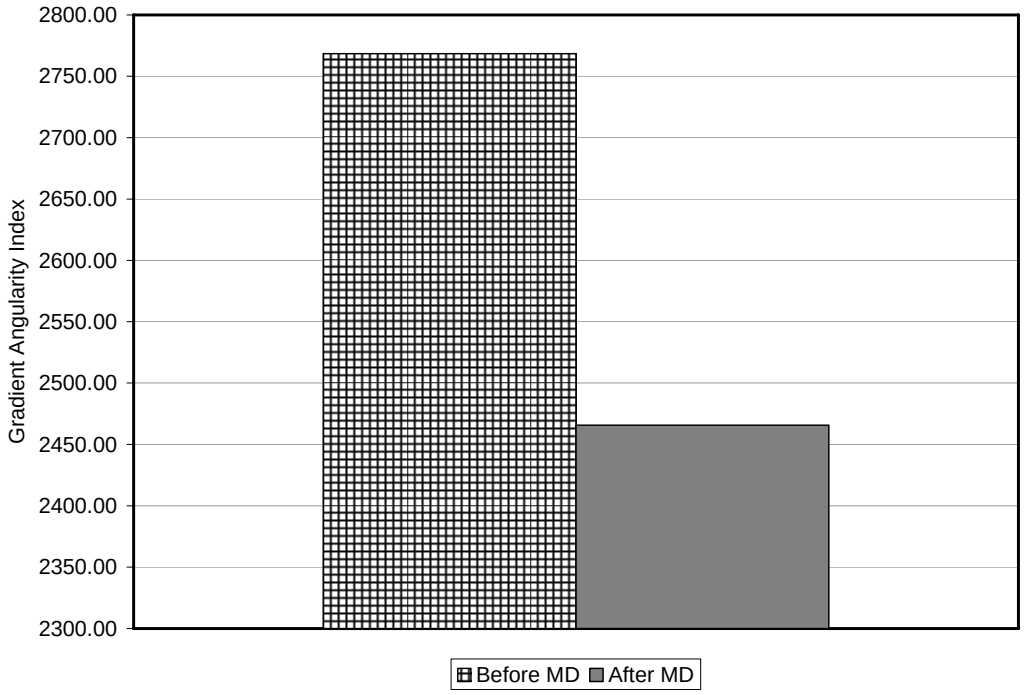

Figure A1-12: AIMS Angularity Results Before and After Micro-Deval Test for Granite.

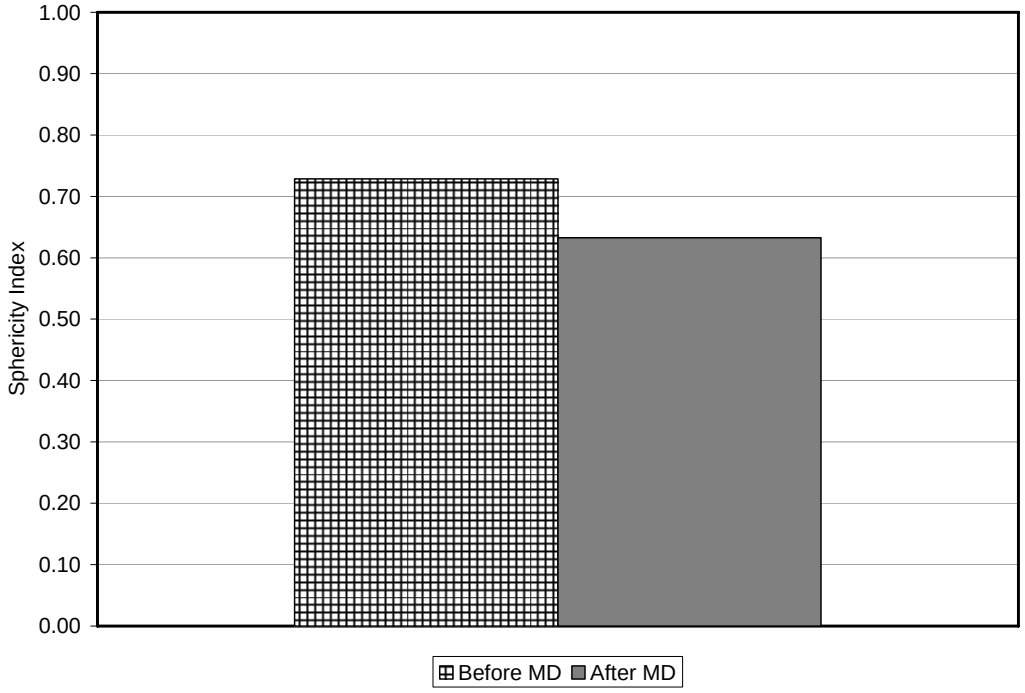

Figure A1-13: AIMS Sphericity Results Before and After Micro-Deval Test for Traprock.

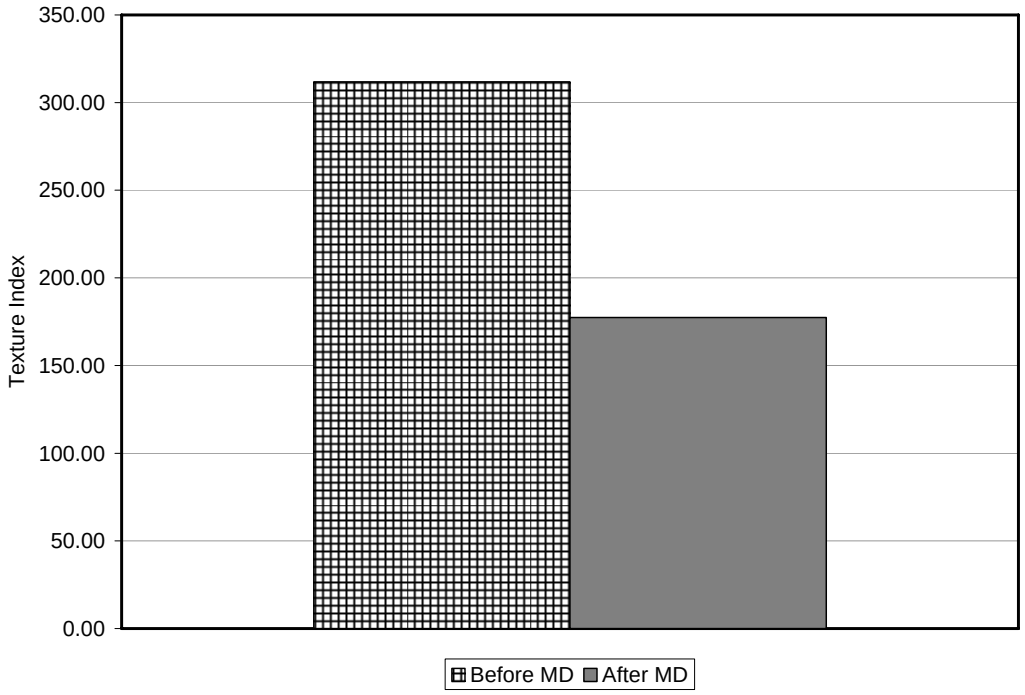

Figure A1-14: AIMS Texture Results Before and After Micro-Deval Test for Traprock.

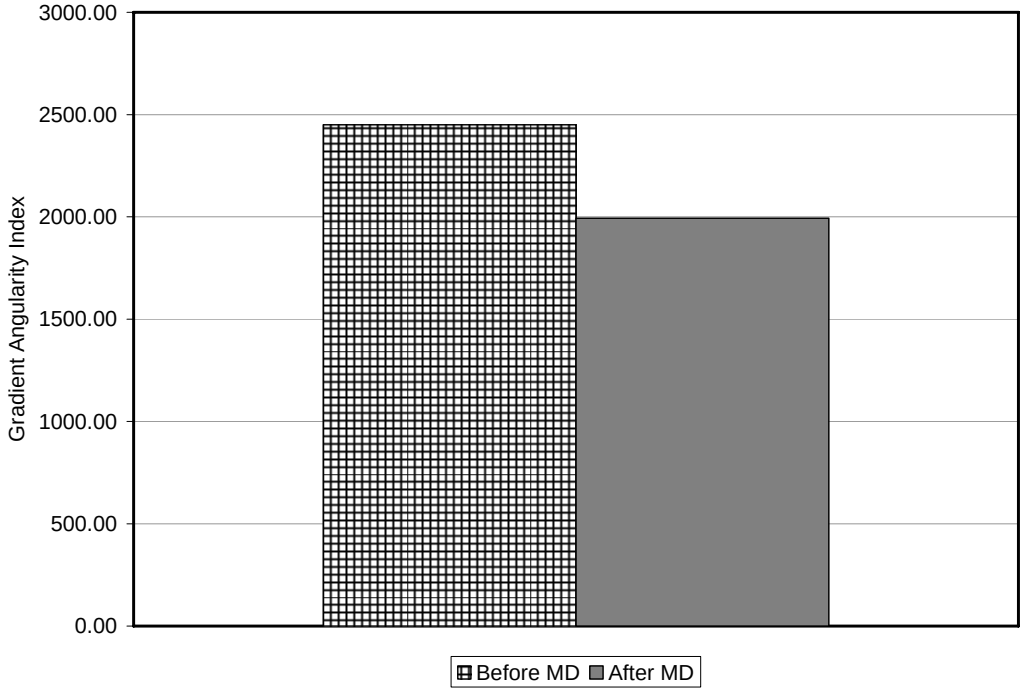

Figure A1-15: AIMS Angularity Results Before and After Micro-Deval Test for Traprock.

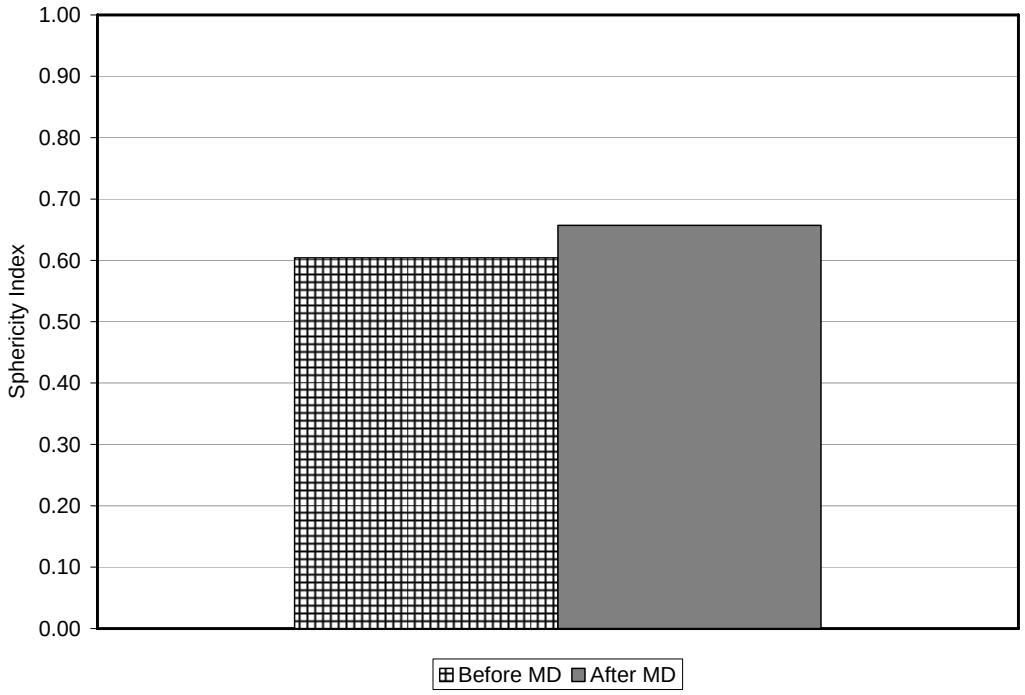

Figure A1-16: AIMS Sphericity Results Before and After Micro-Deval Test for Glacial Gravel.

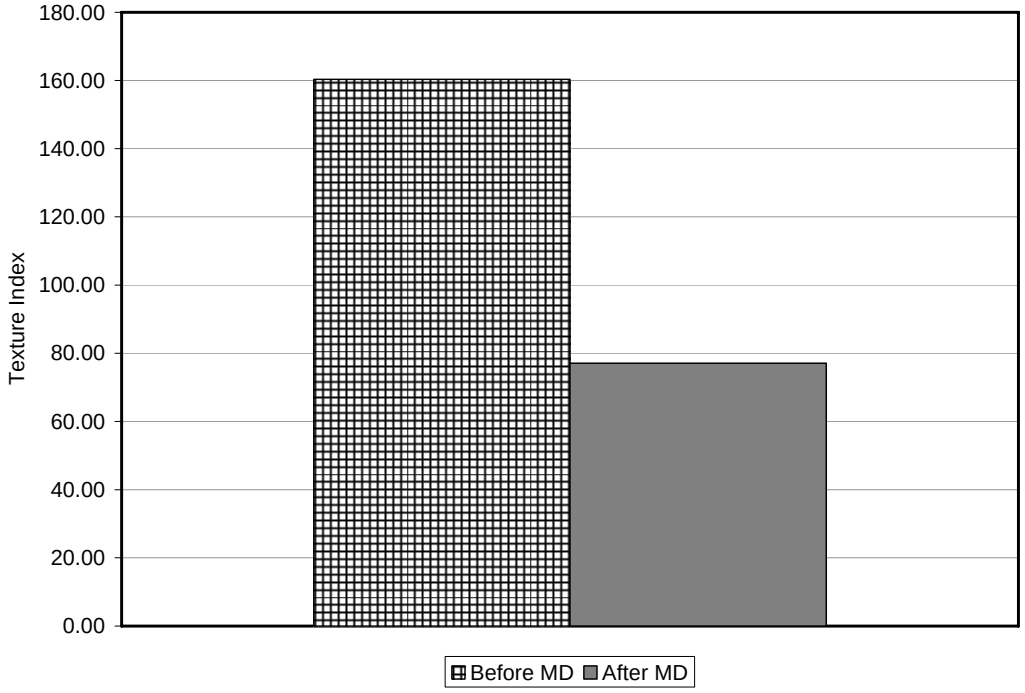

Figure A1-17: AIMS Texture Results Before and After Micro-Deval Test for Glacial Gravel.

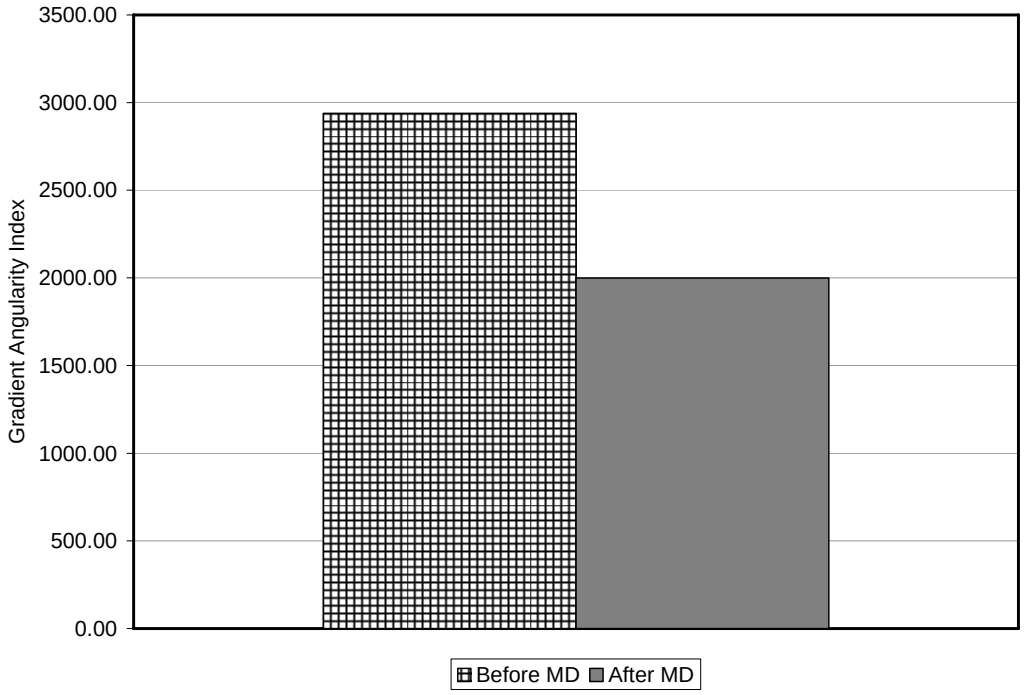

Figure A1-18: AIMS Angularity Results Before and After Micro-Deval Test for Glacial Gravel.

APPENDIX A2

TABLES OF LAB RESULTS FOR THE MECHANICAL SIEVE ANALYSIS

Table A2.1: Sieve Analysis Results for Glacial Gravel.

	Sieve Size, mm	Glacial Gravel Non-compact	Glacial Gravel 100	Glacial Gravel 250	Original
Percent Passing, %	19.05 (3/4")	100	100	100	100
	12.7 (1/2")	88.1	88.0	87.3	89.30
	9.5 (3/8")	62.9	67.8	68.6	59.90
	4.75 (#4)	28.6	32.7	33.4	27.77
	2.36 (#8)	18.3	21.9	22.5	17.92
	1.18 (#16)	15.4	17.0	17.5	14.11
	0.6 (#30)	12.8	13.7	14.3	11.30
	0.3 (#50)	11.4	11.9	12.3	9.71
	0.15 (#100)	10.3	10.6	10.7	8.86
	0.075 (#200)	8.8	9.5	9.3	8.00

Table A2.2: Sieve Analysis Results for Traprock.

	Sieve Size, mm	Traprock Non-Compact	Traprock 100	Traprock 250	Original
Percent Passing, %	19.05 (3/4")	100	100	100	100
	12.7 (1/2")	90.8	89.4	91.0	89.3
	9.5 (3/8")	61.8	67.1	69.3	59.9
	4.75 (#4)	26.3	29.1	28.9	27.77
	2.36 (#8)	17.1	19.0	19.0	17.92
	1.18 (#16)	14.6	16.0	16.0	15.11
	0.6 (#30)	11.9	13.2	13.3	12.3
	0.3 (#50)	10.7	11.7	11.6	10.71
	0.15 (#100)	9.6	10.6	10.5	9.86
	0.075 (#200)	8.1	9.5	9.4	9

Table A2.3: Sieve Analysis Results for Limestone 1.

	Sieve Size, mm	Limestone 1 Non-compact	Limestone 1 100	Limestone 1 250	Original
Percent Passing, %	19.05 (3/4")	100	100	100	100
	12.7 (1/2")	87.9	88.6	91.3	89.3
	9.5 (3/8")	63.0	69.1	73.1	59.9
	4.75 (#4)	27.2	31.5	34.4	27.77
	2.36 (#8)	17.8	23.1	25.6	17.92
	1.18 (#16)	14.0	18.2	20.7	15.11
	0.6 (#30)	11.3	14.9	17.3	12.3
	0.3 (#50)	10.2	13.1	15.4	10.71
	0.15 (#100)	9.1	11.5	13.8	9.86
	0.075 (#200)	7.8	9.9	12.2	9

Table A2.4: Sieve Analysis Results for Limestone 2.

	Sieve Size, mm	Limestone 2 Non-compacted	Limestone 2 100	Limestone 2 250	Original
Percent Passing, %	19.05 (3/4")	100	100	100	100
	12.7 (1/2")	88.3	90.3	87.2	89.3
	9.5 (3/8")	60.5	66.8	67.7	59.9
	4.75 (#4)	27.9	36.3	34.9	27.77
	2.36 (#8)	18.6	24.6	23.7	17.92
	1.18 (#16)	15.9	19.4	19.1	15.11
	0.6 (#30)	13.2	16.8	15.7	12.3
	0.3 (#50)	11.7	15.2	13.6	10.71
	0.15 (#100)	10.7	13.8	11.8	9.86
	0.075 (#200)	9.5	12.3	10.5	9

Table A2.5: Sieve Analysis Results for Granite.

	Sieve Size, mm	Granite Non-compact	Granite 100	Granite 250	Original
Percent Passing, %	19.05 (3/4")	100	100	100	100
	12.7 (1/2")	85.8	88.6	88.2	89.3
	9.5 (3/8")	60.7	63.8	65.0	59.9
	4.75 (#4)	25.8	27.7	28.2	27.77
	2.36 (#8)	17.1	19.0	19.6	17.92
	1.18 (#16)	14.4	15.4	16.0	15.11
	0.6 (#30)	11.9	12.9	13.4	12.3
	0.3 (#50)	10.7	11.5	11.7	10.71
	0.15 (#100)	9.7	10.4	10.4	9.86
	0.075 (#200)	8.5	9.4	8.9	9

Table A2.6: Sieve Analysis Results for Uncrushed River Gravel.

	Sieve Size, mm	River Gravel Non-Compacted	River Gravel 100	River Gravel 250	Original
Percent Passing, %	19.05 (3/4")	100	100	100	100
	12.7 (1/2")	88.7	88.5	87.2	89.3
	9.5 (3/8")	61.0	64.6	65.2	59.9
	4.75 (#4)	27.7	30.6	30.8	27.77
	2.36 (#8)	17.5	20.4	20.7	17.92
	1.18 (#16)	15.0	16.8	17.2	15.11
	0.6 (#30)	12.3	13.8	14.0	12.3
	0.3 (#50)	11.2	11.8	12.0	10.71
	0.15 (#100)	10.4	10.2	10.2	9.86
	0.075 (#200)	9.4	8.61	8.6	9

APPENDIX A3

TABLES DEPICTING DATA OBTAINED FROM THE CONTACT ENERGY INDEX AND SERVOPAC GYRATORY COMPACTOR

Table A3.1: CEI Results for Uncrushed River Gravel.

	Description	C- THE CONTACT ENERGY INDEX (CEI) =	Starting No. of gyration N_{G1} =	Ending No. of gyration N_{G2} =
1	90604	18.443	20	220
2	90605	19.536	18	218
3	90606	19.541	17	217
4	90607	21.314	16	216
	AVERAGE:	19.708	17.75	217.75

Table A3.2: CEI Results for Granite.

	Description	C- THE CONTACT ENERGY INDEX (CEI) =	Starting No. of gyration N_{G1} =	Ending No. of gyration N_{G2} =
1	90392	20.672	24	224
2	90393	20.513	23	223
3	90394	20.184	24	224
4	90395	21.306	22	222
	AVERAGE:	20.669	23.25	223.25

Table A3.3: CEI Results for Crushed Glacial Gravel.

	Description	C- THE CONTACT ENERGY INDEX (CEI) =	Starting No. of gyration N_{G1} =	Ending No. of gyration N_{G2} =
1	90429	21.083	33	233
2	90430	23.758	26	226
3	90431	18.955	39	239
4	90432	19.970	35	235
	AVERAGE:	20.942	33.25	233.25

Table A3.4: CEI Results for Traprock.

	Description	C- THE CONTACT ENERGY INDEX (CEI) =	Starting No. of gyration N_{G1} =	Ending No. of gyration N_{G2} =
1	90398	17.030	28	228
2	90399	18.618	24	224
3	90400	15.844	30	230
4	90401	18.074	22	222
	AVERAGE:	17.391	26	226

Table A3.5: CEI Results for Limestone 1.

	Description	C- THE CONTACT ENERGY INDEX (CEI) =	Starting No. of gyration N_{G1} =	Ending No. of gyration N_{G2} =
1	90583	18.717	37	237
2	90584	22.267	25	225
3	90585	18.820	37	237
4	90586	20.695	30	230
	AVERAGE:	20.125	32.25	232.25

Table A3.6: CEI Results for Limestone 2.

	Description	C- THE CONTACT ENERGY INDEX (CEI) =	Starting No. of gyration N_{G1} =	Ending No. of gyration N_{G2} =
1	90306	19.411	37	237
2	90348	20.130	35	235
	AVERAGE:	19.770	36	236

Table A3.6: Sample Data of Shear Stress Obtained from SGC.

	Shear stress (lab)					
Gyration	**River Gravel**	**Glacial Gravel**	**Granite**	**Traprock**	**Limestone 1**	**Limestone 2**
1	172.75	147.75	147.50	169.25	155.50	143.50
2	270.50	245.00	244.75	274.25	254.00	245.00
3	302.00	286.50	287.00	310.25	296.50	286.00
4	321.75	311.00	309.00	329.00	321.25	314.00
5	333.75	329.00	325.00	340.50	336.25	332.50
6	347.00	341.75	337.75	349.00	347.75	347.50
7	355.75	352.00	347.00	355.00	358.25	358.50
8	364.50	361.00	353.50	361.25	365.50	369.00
9	373.00	368.50	360.25	368.00	372.00	378.00
10	378.00	375.25	365.00	372.75	378.75	385.00
11	383.00	382.50	370.25	375.50	383.75	391.00
12	387.00	389.25	375.75	376.50	389.00	397.50
13	390.75	394.25	379.00	379.75	393.25	403.00
14	394.50	397.75	380.75	382.00	396.00	408.50
15	399.25	401.00	384.25	384.75	399.25	413.00
16	399.75	405.25	386.50	388.50	403.25	417.00
17	403.00	409.00	389.25	390.75	405.75	421.50
18	404.25	412.00	391.75	391.00	408.50	425.50
19	407.50	413.75	394.75	391.50	411.50	428.50
20	409.25	416.25	396.00	392.75	414.25	430.50
21	411.50	418.25	398.50	394.00	417.50	432.50
22	413.50	421.50	401.25	394.50	419.75	435.00
23	415.25	424.50	402.50	396.25	422.50	437.00
24	417.50	426.50	403.00	396.50	424.50	438.50
25	417.75	429.00	404.25	397.50	426.50	441.00
26	419.00	430.50	406.00	398.00	427.75	442.50
27	420.75	432.50	408.00	398.75	429.00	445.50
28	421.50	434.50	408.00	400.00	431.75	449.00
29	422.50	436.00	408.25	401.25	434.00	450.50
30	423.25	437.50	409.25	400.75	435.75	452.00
31	424.50	439.00	410.25	400.75	438.00	454.00
32	425.00	441.00	411.25	400.25	440.50	457.00
33	424.25	442.25	411.00	400.75	442.00	459.00
34	425.00	444.00	410.75	401.00	443.50	461.00
35	425.75	445.50	412.25	402.25	444.50	463.00
36	426.50	447.00	412.50	402.00	445.75	465.00
37	426.50	447.50	413.25	403.00	447.00	466.00
38	425.50	448.25	414.00	403.25	447.75	468.00
39	427.00	449.00	414.50	404.50	447.25	469.00
40	428.25	449.75	415.50	405.00	448.25	470.50
41	428.25	450.75	414.75	405.25	449.00	472.50

	Shear stress (lab)					
Gyration	**River Gravel**	**Glacial Gravel**	**Granite**	**Traprock**	**Limestone 1**	**Limestone 2**
42	428.75	451.75	415.75	406.25	449.25	474.00
43	429.00	452.50	416.25	407.00	450.50	476.00
44	429.75	452.25	416.50	408.00	452.00	476.00
45	431.00	452.75	416.25	407.00	453.00	477.00
46	431.25	453.75	417.50	406.50	453.00	477.50
47	430.75	454.25	416.50	407.25	454.25	478.50
48	431.00	455.00	417.50	406.75	455.00	479.00
49	431.75	455.50	417.25	406.50	455.25	480.00
50	432.00	455.25	418.00	407.00	456.25	480.50
51	432.75	455.75	418.25	407.00	457.25	481.00
52	431.50	456.25	418.00	407.25	457.00	481.00
53	432.00	456.00	418.50	408.25	457.25	480.00
54	432.75	456.00	418.75	409.25	458.00	481.00
55	432.50	457.00	419.00	409.50	458.25	480.00
56	432.50	457.50	420.25	409.25	457.50	482.50
57	433.00	457.50	419.50	409.25	458.25	482.50
58	434.00	458.00	419.25	409.50	457.75	483.50
59	434.25	458.50	420.00	409.50	458.25	484.00
60	435.50	459.00	420.00	408.75	457.75	483.50
61	434.25	459.50	419.25	408.50	457.75	483.00
62	435.25	459.25	418.50	408.75	459.25	483.50
63	435.00	460.25	419.00	408.50	459.25	483.50
64	433.50	460.25	418.00	409.00	459.25	483.00
65	434.25	461.00	417.25	408.50	460.50	482.50
66	434.00	461.50	417.00	408.50	460.50	482.50
67	433.75	461.75	417.00	408.75	460.00	483.00
68	434.50	462.00	416.75	408.50	459.00	484.00
69	434.25	462.75	417.75	408.75	460.25	483.50
70	434.50	462.25	416.75	408.00	459.50	483.00
71	433.75	462.25	416.50	408.25	460.00	481.50
72	433.50	462.50	416.50	408.75	460.25	481.50
73	433.50	461.75	416.00	409.25	459.75	481.00
74	434.75	461.50	416.00	409.50	459.75	481.50
75	435.00	462.00	415.75	409.25	459.50	482.50
76	435.00	462.00	415.50	409.75	459.50	482.00
77	434.75	462.25	415.00	409.25	459.75	481.00
78	434.25	462.75	415.25	408.75	459.75	480.00
79	433.50	463.25	415.00	409.25	460.75	480.50
80	434.25	464.00	415.00	409.50	460.50	480.00
81	434.25	463.00	415.25	409.25	460.50	479.50
82	433.25	463.25	415.25	409.25	460.75	478.50
83	433.00	463.50	415.25	408.75	461.00	478.50
84	433.00	463.50	415.50	408.75	461.00	477.50

APPENDIX A4

FIGURES DEPICTING DATA OBTAINED FROM THE X-RAY CT ANALYSIS

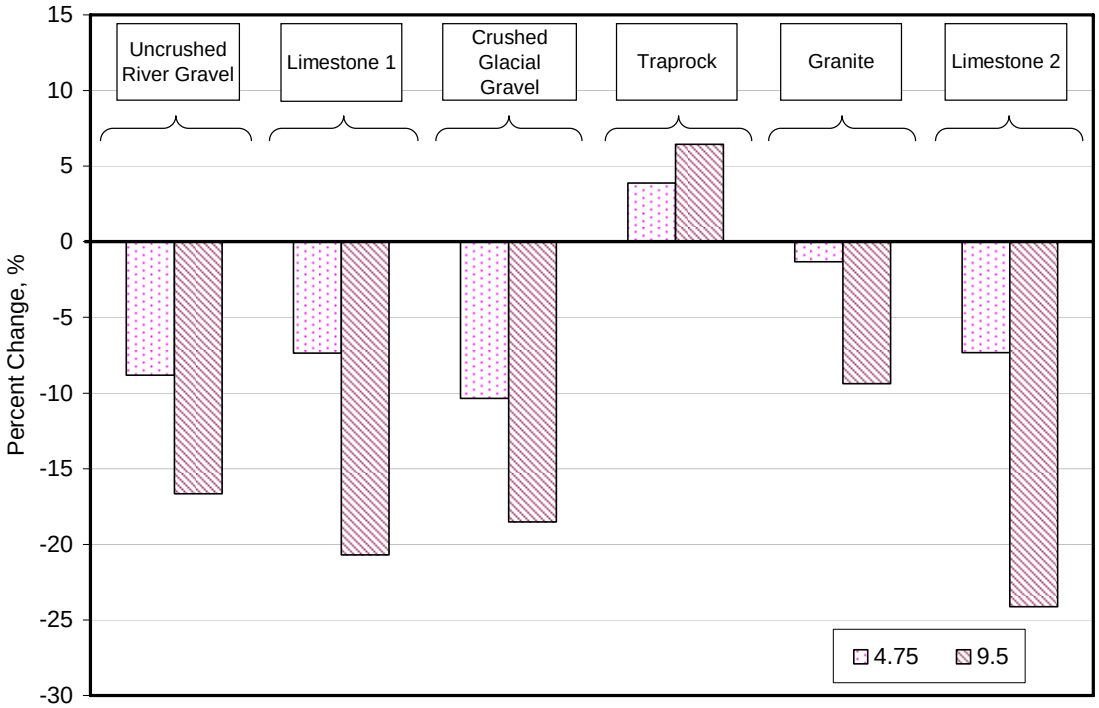

Figure A4.1: 25th Percentile of Change in Gradation of X-Ray CT Analysis.

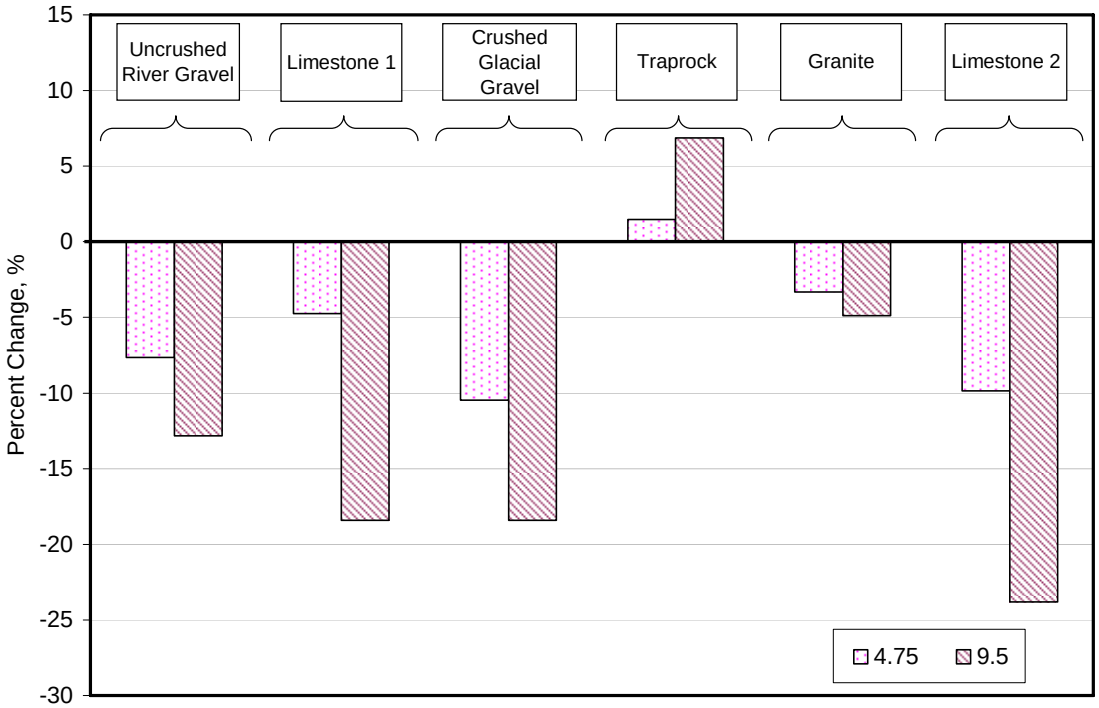

Figure A4.2: 75th Percentile of Change in Gradation of X-Ray CT Analysis.

APPENDIX A5

TABLE OF GRADATION DATA OBTAINED FROM THE MECHANICAL SIEVE ANALYSIS OF THE FLOW NUMBER TEST SPECIMENS

Table A5.1: Gradation Results from Flow Number Test for Granite.

Percent Passing, %	Sieve Size, mm	Granite	
		Before Flow #	After Flow #
	19.05 (3/4")	100.0	100.0
	12.7 (1/2")	92.9	91.6
	9.5 (3/8")	63.7	67.6
	4.75 (#4)	31.7	31.9
	2.36 (#8)	21.1	21.3
	1.18 (#16)	17.3	17.2
	0.6 (#30)	14.2	14.8
	0.3 (#50)	12.3	13.4
	0.15 (#100)	10.8	12.2
	0.075 (#200)	9.22	10.87

Table A5.2: Gradation Results from Flow Number Test for Uncrushed River Gravel.

Percent Passing, %	Sieve Size, mm	Uncrushed River Gravel	
		Before Flow #	After Flow #
	19.05 (3/4")	100.0	100.0
	12.7 (1/2")	90.8	90.7
	9.5 (3/8")	67.9	67.7
	4.75 (#4)	34.9	32.9
	2.36 (#8)	20.6	20.5
	1.18 (#16)	17.4	17.2
	0.6 (#30)	14.4	14.4
	0.3 (#50)	12.9	12.8
	0.15 (#100)	11.8	11.8
	0.075 (#200)	10.46	10.48

Table A5.3: Gradation Results from Flow Number Test for Glacial Gravel.

Percent Passing, %	Sieve Size, mm	Glacial Gravel	
		Before Flow #	After Flow #
	19.05 (3/4")	100.0	100.0
	12.7 (1/2")	89.7	90.7
	9.5 (3/8")	68.0	68.2
	4.75 (#4)	34.9	34.5
	2.36 (#8)	23.3	22.1
	1.18 (#16)	18.1	16.5
	0.6 (#30)	14.7	13.3
	0.3 (#50)	12.7	11.5
	0.15 (#100)	11.4	10.1
	0.075 (#200)	10.04	8.82

Table A5.4: Gradation Results from Flow Number Test for Traprock.

Percent Passing, %	Sieve Size, mm	Traprock	
		Before Flow #	After Flow #
	19.05 (3/4")	100.0	100.0
	12.7 (1/2")	91.2	90.2
	9.5 (3/8")	67.2	68.0
	4.75 (#4)	30.6	29.8
	2.36 (#8)	19.9	19.5
	1.18 (#16)	16.6	16.5
	0.6 (#30)	13.7	13.6
	0.3 (#50)	12.1	11.9
	0.15 (#100)	10.8	10.5
	0.075 (#200)	9.33	8.84

Table A5.5: Gradation Results from Flow Number Test for Limestone 1.

Percent Passing, %	Sieve Size, mm	Limestone 1	
		Before Flow #	After Flow #
	19.05 (3/4")	100.0	100.0
	12.7 (1/2")	90.1	90.6
	9.5 (3/8")	68.3	67.1
	4.75 (#4)	34.4	33.7
	2.36 (#8)	23.7	23.3
	1.18 (#16)	18.9	18.8
	0.6 (#30)	15.6	15.4
	0.3 (#50)	13.7	13.8
	0.15 (#100)	12.4	12.6
	0.075 (#200)	10.81	11.14

Table A5.6: Gradation Results from Flow Number Test for Limestone 2.

Percent Passing, %	Sieve Size, mm	Limestone 2	
		Before Flow #	After Flow #
	19.05 (3/4")	100.0	100.0
	12.7 (1/2")	90.8	92.3
	9.5 (3/8")	69.4	71.5
	4.75 (#4)	36.7	38.1
	2.36 (#8)	24.1	24.5
	1.18 (#16)	19.9	20.2
	0.6 (#30)	16.5	16.9
	0.3 (#50)	14.4	14.8
	0.15 (#100)	13.0	13.3
	0.075 (#200)	11.18	11.66